Doctoral Thesis

Studies on Synthesis, Structure, and Properties of π-Stacked Poly(dibenzofulvene)

(π–スタック型ポリ(ジベンゾフルベン)の合成、構造および性質に関する研究)

Hassan Nageh（ナゲ　ハッサン）

Macromolecular Science Research Division

Institute for Catalysis

Hokkaido University

Table of Contents

Chapter 1
General Introduction

Control over spatial arrangement of π-electronic groups is an important goal in designing functional polymeric materials because it significantly affects performances of π-electronic polymers and molecular systems exhibiting photo electronic properties such as conduction, emission, optical non-linearity optical, and even photo catalytic activity.[1] Such properties and functions are based on electronic or energetic interactions in the π-conjugated systems, within a molecule and between molecules. It is hence important to design a polymer system so a charge or energy can be transported/transferred smoothly in a regulated way.

The most successful and practical examples in this discipline are main-chain conjugated polymers represented by polyacetylene whose conduction has been ascribed to mobility of charged injected by doping through a conjugated chain and among chains. Since the finding of conduction of polyacetylene by Shirakawa, Heeger, and MacDiarmid (The Nobel Prize in Chemistry 2000),[2] various main-chain conjugated polymers have been designed and synthesized, among which poly(3,4-ethylenedioxythiophene) (PEDOT) in combination of poly(styrenesulfonate) (PSS) is one of the most industrially applied example.[3] With the excellent conduction behaviors of main-chain conjugated polymers, they have drawbacks including deep color, poor solubility, and chemical fragileness through oxidation. These drawbacks are inherent to the long main-chain conjugation: a narrow HOMO-LUMO levels gap due to the long conjugation allows photoexcitation by visible light, rigidity of the polymer chain arising from limited rotation freedom of bonds that constitute the long main-chain conjugation system promotes inter-chain interactions, and oxidation by O_2 in the air deteriorating electronic properties rather easily occurs due to relatively high HOMO levels.

These aspects can be overcome through an alternative π-electronic macromolecular

design, a π-stacked structure. A stack of aromatic groups is an ideal structural motif where charge transport and energy transfer are realized.

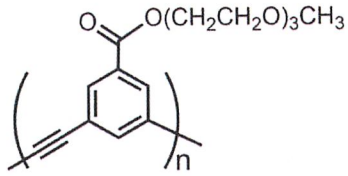

Oligo(*m*-phenyleneethynylene)

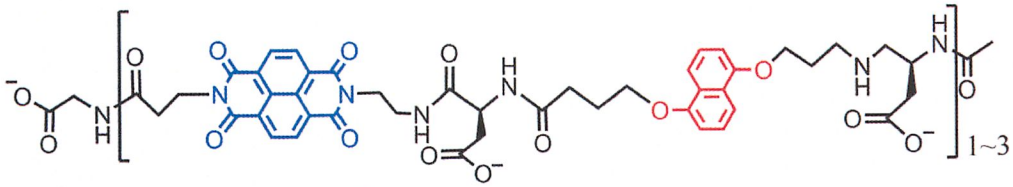

Donor-acceptor oligomer

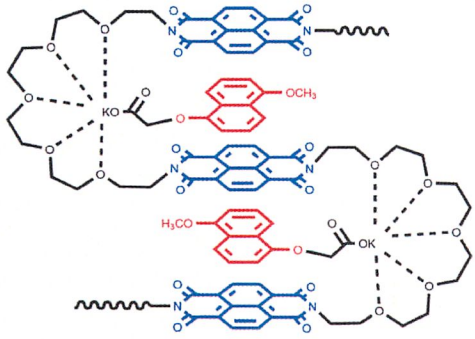

Acceptor oligomer interacting with donor

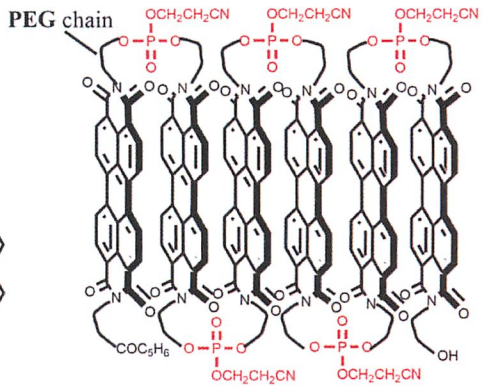

Oligomer having perylene moieties

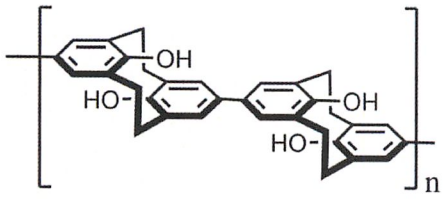

Polymer containing cyclophane units

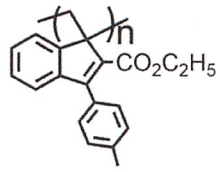

Benzfulvene polymer

Poly(**DBF**)

Figure 1.1. Structure of π-stacked polymers.

Piling up multiple aromatic groups without forming covalent bonds among them in an orderly stack in a polymer system may create novel photo electronic polymeric materials free from the shortcomings noted above and even with improved properties. Based on this idea, artificial π-stacked polymeric and molecular systems have been designed **(Figure 1.1)**; the examples include oligo(*m*-phenyleneethynylene)s,[4] oligomers consisting of alternating donor and acceptor monomeric units,[5,6] oligomers consisting of acceptor monomeric units in the main chain that interact with a low-molecular-weight donor molecule,[7] oligomers having perylene moieties in the main chain,[8,9] polymers consisting of cyclophane units,[10–12] a polymer of bezofulvene derivative,[13,14] and polymers of dibenzofulvene (DBF) and its derivatives.[15-23] Among these examples, poly(dibenzofulvene) (poly(DBF)) is the first, π-stacked vinyl polymer. In this work, in order to expand and deepen the synthetic and structural aspects of poly(DBF), monomer and polymer syntheses were studied from views that had never been assessed. In addition, solid-state structure of poly(DBF) was examined for the first time by means of various analytical methods. This thesis summarizes and discusses these aspects and comprises of four chapters. Chapter 1 introduces the background information, Chapter 2 describes a novel method of the synthesis of DBF monomer which is based on photo excited-state chemistry, Chapter 3 discusses the cationic polymerization of DBF which leads to a new π-stacked structure which have been unforeseen in the anionic[15,16] and radical[18] polymerizations, and Chapter 4 explores into the solid-state structure of poly(DBF) where chain alignments were found.

References

1 T. Nakano, π-Stacked Polymers and Molecules, Springer, 2016.

2 (a) C. K. Chiang, C. R. Fincher Jr, Y. W. Park, A. J. Heeger, H. Shirakawa, E. J. Louis, S. C. Gau and A. G. MacDiarmid, Electrical conductivity in doped polyacetylene,

Phys. Rev. Lett. 1977, **39**, 1098-1101; (b) H. Shirakawa, E. J. Louis, A. G. MacDiarmid, C. K. Chiang and A. J. Heeger, Synthesis of electrically conducting organic polymers: halogen derivatives of polyacetylene,$(CH)_x$, J. Chem. Soc., Chem. Commun., 1977, 578-580; (c) H. Shirakawa, A. McDiarmid and A. Heeger, Twenty-five years of conducting polymers, Chem. Commun., 2003, 1-4.

3 (a) F. Jonas, W. Kraft, US Patent No. 5 300 575; (b) G. Heywang and F. Jonas, Poly(alkylenedioxythiophene) s—new, very stable conducting polymers, Adv. Mater., 1992, **4**, 116-118; (c) A. Aleshin, S. Williams and A. Heeger, Transport properties of poly(3,4-ethylenedioxythiophene)/poly(styrenesulfonate), Synth. Met., 1998, **94**, 173-177. (d) Y. Cao, G. Yu, C. Zhang, R. Menon and A. Heeger, Polymer light-emitting diodes with polyethylene dioxythiophene–polystyrene sulfonate as the transparent anode, Synth. Met., 1997, **87**, 171-174; (e) J. Scott, S. Carter, S. Karg and M. Angelopoulos, Polymeric anodes for organic light-emitting diodes, Synth. Met., 1997, **85**, 1197-1200.

4 J. C. Nelson, J. G. Saven, J. S. Moore and P. G. Wolynes, Solvophobically driven folding of nonbiological oligomers, Science, 1997, **277**, 1793–1796.

5 R. S. Lokey and B. L. Iverson, Synthetic molecules that fold into a pleated secondary structure in solution, Nature, 1995, **375**, 303–305.

6 J. Q. Nguyen and B. L. Iverson, An amphiphilic folding molecule that undergoes an irreversible conformational change, J. Am. Chem. Soc., 1999, **121**, 2639–2640.

7 S. G. Ramkumar and S. Ramakrishnan, Understanding the folding process of synthetic polymers by small-molecule folding agents, J. Chem. Sci., 2008, **120**, 187–194.

8 W. Wang, L.- S. Li, G. Helms, H.- H. Zhou and A. D. Q. Li, To fold or to assemble?, J. Am. Chem. Soc., 2003, **125**, 1120–1121.

9 J. J. Han, A. D. Shaller, W. Wang and A. D. Q. Li, Architecturally diverse nanostructured foldamers reveal insightful photoinduced single-molecule dynamics, J.

Am.Chem. Soc., 2008, **130**, 6974–6982.

10 S. Mizogami and S. Yoshimura, Synthesis of a new polyconjugated system: polycyclophane. J. Chem. Soc. Chem. Commun., 1985, 427–428.

11 S. Mizogami and S. Yoshimura, Synthesis of a new crystalline polymer: polymetacyclophane, J. Chem. Soc., Chem. Commun., 1985, 1736–1738.

12 Y. Morisaki and Y. Chujo, Through-space conjugated polymers based on cyclophanes, Angew. Chem. Int. Ed., 2006, **45**, 6430–6437.

13 A. Cappelli, G. P. Pericot Mohr, M. Anzini, S. Vomero, A. Donati, M. Casolaro, R. Mendichi, G. Giorgi and F. Makovec, Synthesis and characterization of a new benzofulvene polymer showing a thermoreversible polymerization behavior, J. Org. Chem., 2003, **68**, 9473–9476.

14 A. Cappelli, S. Galeazzi, G. Giuliani, M. Anzini, M. Aggravi, A. Donati, L. Zetta, A. C. Boccia, R. Mendichi, G. Giorgi, E. Paccagnini and S. Vomero, Anionic polymerization of a benzofulvene monomer leading to a thermoreversible π-stacked polymer. Studies in macromolecular and aggregate structure, Macromolecules, 2008, **41**, 2324–2334.

15 T. Nakano, K. Takewaki, T. Yade and Y. Okamoto, Dibenzofulvene, a 1,1-diphenylethylene analogue, gives a π-stacked polymer by anionic, free-radical, and cationic catalysts, J. Am. Chem. Soc., 2001, **123,** 9182-9183.

16 T. Nakano, and T. Yade, Synthesis, structure, and photophysical and electrochemical properties of a π-stacked polymer, J. Am. Chem. Soc., 2003**, 125**, 15474-15484.

17. T. Nakano, T. Yade, M. Yokoyama and N. Nagayama, Charge Transport in a π-Stacked Poly (dibenzofulvene) Film, Chem. Lett., 2004, **33**, 296-297.

18 T. Nakano, T. Yade, Y. Fukuda, T. Yamaguchi and S. Okumura, Free-radical polymerization of dibenzofulvene leading to a π-stacked polymer: structure and properties of the polymer and proposed reaction mechanism, Macromolecules, 2005, **38**, 8140-8148.

19. V. Coropceanu, T. Nakano, N. E. Gruhn, O. Kwon, T. Yade, K. Katsukawa and J. L. Bredas, Probing charge transport in π-stacked fluorene-based systems, J. Phys. Chem. B, 2006, **110**, 9482-9487.

20 T. Nakano, M. Tanikawa, O. Nakagawa, T. Yade and T. Sakamoto, Synthesis and structure of an optically active π-stacked poly (dibenzofulvene) bearing chiral terminal group, J. Polym. Sci., Part A: Polym. Chem., 2009, **47**, 239-246.

21 T. Nakano, Synthesis, structure and function of π-stacked polymers, Polym. J., 2010, **42**, 103-123.

22 K. Watanabe, T. Sakamoto, M. Taguchi, M. Fujiki and T. Nakano, A chiral π-stacked vinyl polymer emitting white circularly polarized light, Chem. Commun., **47**, 10996-10998.

23 H. Nageh, Y. Wang and T. Nakano, Cationic polymerization of dibenzofulvene leading to a π-stacked polymer, Polymer, 2018, **144**, 51-56.

Chapter 2

Photo-induced β-elimination of 9-fluorenylmethanol leading to dibenzofulvene

2.1 Introduction

Photochemistry is an important discipline in organic synthesis because light promotes various reactions which are not driven by heat.[1] Typical elemental reactions induced by light include *E–Z* isomerization, bond scission leading to radicals or carbene, ring closure and cycloaddition. Although various products have been obtained through these photochemical reactions, a clean, photo-induced dehydration (β-elimination) of alcohols leading to olefins in the absence of side reactions is unprecedented. Because olefins can be used as source materials for functional vinyl polymers, their synthesis through alcohol dehydration is as important as the other methods, including the aldol condensation,[2] Wittig reaction,[3] Tebbe-reagent-based olefination,[4] Peterson olefination,[5] Julia–Lythgoe olefination,[6] McMurry reaction (carbonyl coupling),[7] Shapiro and related reactions,[8] and hydrogenation of acetylenes.[9] In the ground state, the dehydration of alcohols can be achieved by β-elimination through contact with a base or an acid.

Herein we report the first, efficient photo-induced β-elimination of alcohol to olefin through a radical-mediated mechanism which converts 9-fluorenylmethanol (FM) to dibenzofulvene (DBF) **(Scheme 2.1)**.

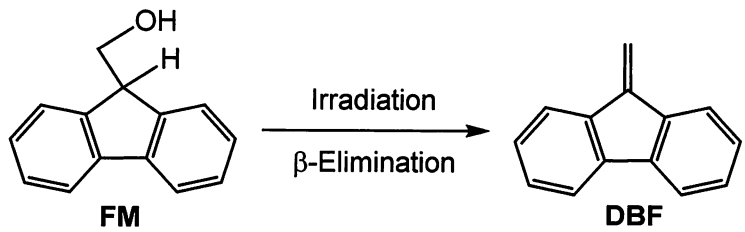

Scheme 2.1. Synthesis of dibenzofulvene (DBF) through photo-induced β-elimination of 9-fluorenylmethanol (FM).

DBF is an important olefin that leads through vinyl polymerization to poly(DBF) having a unique π-stacked conformation.[10] On the basis of the conformation, the polymer exhibits characteristic photoelectronic properties such as high charge mobility and remarkable hypochromism as well as charge delocalization over the stacked fluorene units. DBF monomers have been synthesized in the ground state from FM in the presence of a base such as *t*-BuOK where dehydration is considered to occur through an E1cb mechanism.[11] The present study discloses that DBF is obtained in the absence of base upon photoirradiation and proposes that the reaction occurs through β-elimination via a radical-mediated mechanism.

2.2 Experimental

2.2.1 Materials

9-Fluorenylmethanol (FM) (TCI), potassium t-butoxide (TCI) and 2,2,6,6-tetramethyl4-piperidinol (Sigma-Aldrich) were used as obtained. Hexane (Kanto) was washed with conc. H_2SO_4, aq. NaOH, and water in this order and distilled over CaH_2 under N_2. Methanol (Kanto) was distilled over CaH_2 under N_2. Acetonitrile (Kanto) was dried on MS4A and distilled under N_2. Distilled H_2O was obtained through the purified water supply system at Institute for Catalysis, Hokkaido University. Dibenzofulvene (DBF), the pristine sample, was synthesized according to the literature.[10]

2.2.2 Instrumentation and measurements

NMR spectra were recorded on JEOL JNM-ESC400 spectrometer (400 MHz for ^1H, 100 MHz for ^{13}C). Size-exclusion chromatography (SEC) measurements were carried out using a chromatographic system consisting of a JASCO DG-980- 50 degasser, a HITACHI L-7100 pump, a HITACHI L-7420 UV-Vis detector and a HITACHI L7490 RI detector, equipped with TOSOH TSKgel G3000H HR and G6000H HR columns (30

× 0.72 (i.d.) cm) connected in series (eluent: THF, flow rate: 1.0 mL/min). UV-Vis spectra were taken in quartz cells on JASCO V-550 and V-570 spectrophotometers, and fluorescence spectra were measured using quartz cells on a JASCO PF-8500 fluorescence spectrophotometer. FT-IR spectra were recorded on a JASCO FT/IR-6100 apparatus. Photo irradiation was conducted using a 300-W Xe lamp (Cermax Y-1089) in a R300-3J lamp house driven with a model CX-04E power source with a MR 60/90-ALM 45-deg reflecting mirror unit equipped with a CM2 UV cold mirror, an Asahi Spectra 1200 50x50 cold filter, and a quartz-made focus lens.

2.2.3. Irradiation experiments

Solutions at 3.9 x 10^{-5} M were prepared in the following manner (samples for the data in **Table 2.1**). A hexane solution of FM at 3.9 x 10^{-5} M was prepared as follows (a sample for the data in **Table 2.1**). A hexane solution: a 10-mL solution of FM in hexane (3.78 mg, 1.9 x 10^{-3} M) was prepared in a volumetric flask from which a 2-mL portion was transferred using a 2-mL graduated pipette to a 100-mL volumetric flask where a solution at 3.9 x 10^{-5} M in hexane was made by dilution. A methanol solution: a 10-mL solution of FM in methanol (0.41 mg, 2.1 x 10^{-4} M) was prepared in a volumetric flask from which a 4.6-mL portion was transferred using a 5-mL graduated pipette to a 25-mL volumetric flask where a solution at 4 x 10^{-5} M in methanol was made by dilution. An acetonitrile solution: a 10-mL solution of FM in acetonitrile (1.57 mg, 8.0 x 10^{-4} M) was prepared in a volumetric flask from which a 1.2-mL portion was transferred using a 2-mL graduated pipette to a 25-mL volumetric flask where a solution at 3.9 x 10^{-5} M in acetonitrile was made by dilution. An H_2O solution: a 100-mL solution of FM in H_2O (9.81 mg, 5.0 x 10^{-4} M) was prepared in a volumetric flask from which a 0.77-mL portion was transferred using a 1-mL graduated pipette to a 10-mL volumetric flask where a solution at 3.9 x 10^{-5} M in H_2O was made by dilution. A sample solution in a 1-cm, two-face quartz cell was irradiated for a prescribed duration of time. The distance

between the reflecting mirror and the focusing lens was 15 cm, and that between the lens and the sample cell was 10 cm. A home-made aluminum-foil reflecting chamber was placed behind the cell.

2.2.4. Determination of molar absroptivities of FM in hexane, methanol, acetonitrile, and H_2O

Absorbance values were measured at five to six different concentrations **(Figure 2.7)**, and molar absorptivities were estimated by a linear plot of absorbance against concentration. Sample solutions were prepared as follows and numerical data are summarized in **Table 2.3**. A 100-mL solution of FM (9.81 mg, 5 x 10^{-4} M) was prepared using volumetric flask from which 4.5-mL was transferred using a graduated pipette to a 25-mL volumetric flask to made 9.0 x 10^{-5} M by dilution. A 1.5-mL portion of the 5 x 10^{-4} M solution was transferred to 10-mL volumetric flask to made 7.5 x 10^{-5} M by dilution. A 3-mL portion of 5 x 10^{-4} M solution was transferred using a whole pipette to 25-mL volumetric flask to made 6.0 x 10^{-5} M by dilution. A 1-mL portion of this solution of the 5 x 10^{-4} M solution was transferred to 10-mL volumetric flask to made 5.0 x 10^{-5} M by dilution. A 2-mL portion of the 5 x 10^{-4} M solution was transferred using a graduated pipette to a 25-mL volumetric flask to made 4.0 x 10^{-5} M by dilution. A 3-mL portion of the 5 x 10^{-5} M solution was transferred to 5-mL volumetric flask to made 3 x 10^{-5} M by dilution. A 0.5-mL portion of the 5 x 10^{-4} M solution was transferred using a graduated pipette to a 10-mL volumetric flask to made 2.5 x 10^{-5} M by dilution. A 1-mL portion of 5 x 10^{-5} M solution was transferred using a graduated pipette to 5-mL volumetric flask to made 1 x 10^{-5} M by dilution, and then 1-mL 3 portion of this solution (1 x 10^{-5} M) was transferred using a whole pipette to 10-mL volumetric flask to made 1 x 10^{-6} M by dilution.

2.2.5. Determination of molar absorptivities of DBF in hexane, methanol, and acetonitrile

Molar absorptivities were estimated by absorbance spectra taken in the solvents where one spectrum was taken for each solvent at the concentrations indicated below. Sample solutions were prepared as follows and numerical data are summarized in **Table 2.2**. Molar absorptivity in H_2O was not determined, and the value for methanol was used for the experiments in H_2O. A hexane solution: a 50-mL solution of DBF in hexane (17.75 mg, 1.99×10^{-3} M) was prepared in volumetric flask from which a 1-mL was transferred using a whole pipette to a 100-mL volumetric flask where a solution at 1.99×10^{-5} M was made by dilution. A methanol solution: a 50-mL solution (18.35 mg, 2.06×10^{-3} M) was prepared in volumetric flask from which a 1-mL was transferred using a whole pipette to a 100-mL volumetric flask where a solution at 2.06×10^{-5} M was made by dilution. An acetonitrile solution: A 50-mL solution (15.13 mg, 1.70×10^{-3} M) was prepared in volumetric flask from which a 1-mL was transferred using a whole pipette to a 100-mL volumetric flask where a solution at 1.70×10^{-5} M was made by dilution.

2.2.6. Fluorescence measurements of FM as well as 9,10-diphenylanthracene as a standard compound for emission quantum yield measurements in hexane, methanol, acetonitrile, and H_2O

Sample solutions were prepared as follows and numerical data are summarized in **Table 2.4**. FM solutions: a 100-mL solution of FM (9.81 mg, 5.0×10^{-4} M) was prepared using volumetric flask from which a 1-mL portion was transferred using a 1-mL whole pipette to a 5-mL volumetric flask where a solution at 1.0×10^{-4} M was made by dilution. A 1-mL of this solution (1.0×10^{-4} M) was transferred to a 10-mL volumetric flask and diluted to a solution at 1.0×10^{-5} M. A 1-mL portion of the solution (1.0×10^{-5} M) was transferred to a 10-mL volumetric flask and diluted to a solution at 1.0×10^{-6} M. 9,10-Diphenylanthracene solutions: a 10-mL solution (3.30 mg, 1.0×10^{-3} M) was prepared

using a 10-mL volumetric flask from which a 1-mL portion was transferred using a 1-mL graduated pipette to a 10-mL volumetric flask where a solution at 1.0×10^{-4} M was made by dilution. A 1-mL portion of this solution (1.0×10^{-4} M) was transferred to a 10-mL volumetric flask and diluted to a solution at 1.0×10^{-5} M, and also a 1-mL portion of the solution (1.0×10^{-5} M) was transferred to a 10-mL volumetric flask and diluted to a solution at 1.0×10^{-6} M. Fluorescence spectra were measured on excitation at 265 nm in 1-cm, four-face quartz cell sealed with a screw cap using the solution which had been bubbled with N_2 gas for 20 min.

2.2.7. Computational method

Geometry optimization was carried out with the density functional theory (DFT) calculation with the B3LYP functional. For the basis functions, the 6-31G sets were used for all the atoms. This computational set up is accurate enough to investigate qualitative mechanism of organic reactions. Singlet excited states were calculated using time-dependent density functional theory (TDDFT). For the lowest triplet state, the ground-state DFT with single determinant was used. The Gaussian 09 package was used for the computations. For geometry optimization of the minimum energy intersystem crossing point, our in-house code was used. To connect reactant and product states in triplet-state potential energy surface, the sphere contracting walk method (SCW) was used. To locate some transition states, the scaled hypersphere search method (2PSHS) was used. The SCW and 2SHS calculations were carried out using the GRRM14 package. [14]

2.3 Results and Discussion

Figure 2.1 shows the UV spectral change of a hexane solution of FM upon irradiation (panel A) along with the UV spectrum of pristine DBF (panel B).

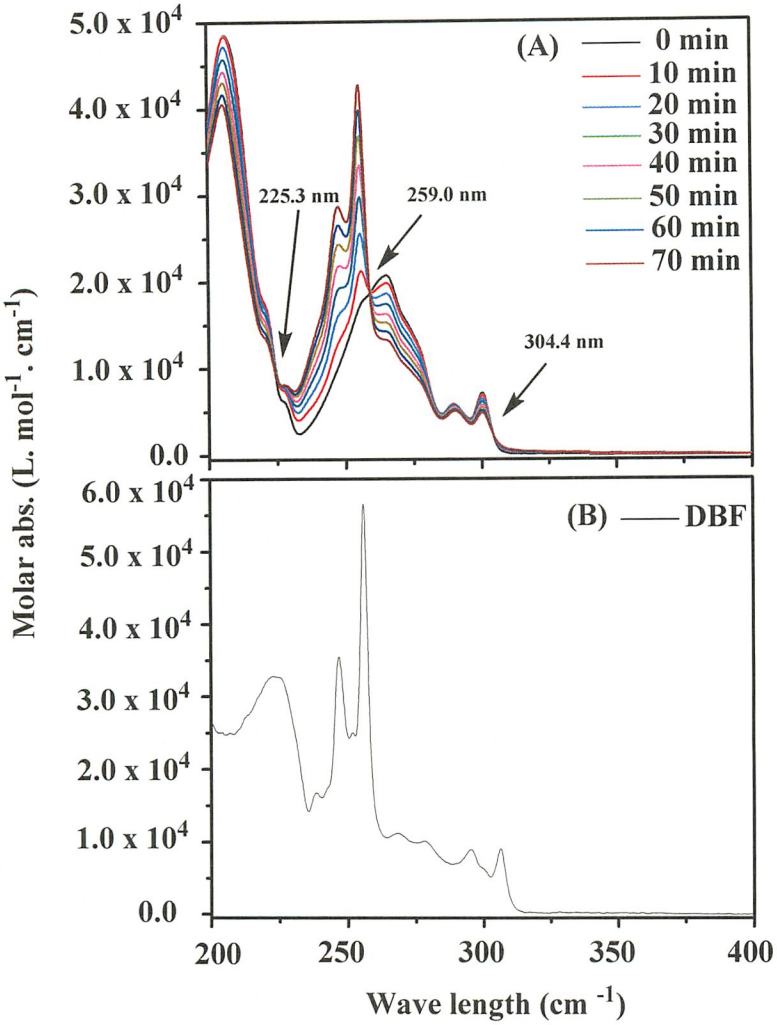

Figure 2.1. UV spectra of a hexane solution of FM observed upon irradiation using a 300 W Xe lamp (A) ($[FM]_0$ = 1.6 x 10^{-5} M), (cell path = 1 cm) and UV spectrum of pristine DBF in hexane (B) ([DBF] = 2.0 x 10^{-5} M, cell path = 1 cm).

Upon irradiation, the signals due to DBF appeared and they became more intense with an increase in irradiation time at the cost of the signals due to FM. The presence of clear isosbestic points at 225 nm, 259 nm, and 304 nm indicates that the reaction system contains only FM and DBF and that no side reaction occurred upon irradiation. The production of DBF in hexane upon irradiation was further confirmed by the IR spectrum (**Figure 2.2**).

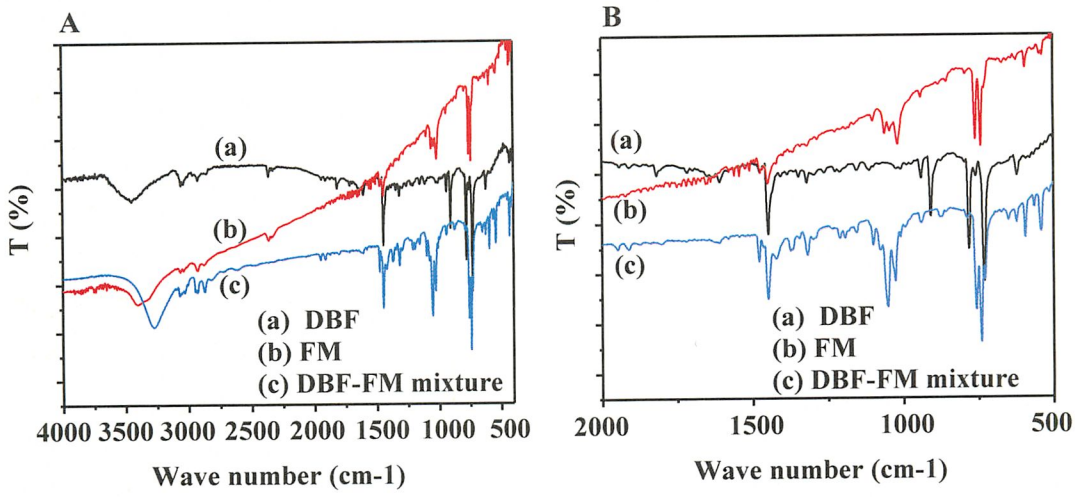

Figure 2.2. IR spectra of DBF (a), FM (b) and a photo-generated DBF-FM mixture (c) prepared in hexane (3.9 x 10^{-5} M) on irradiation for 70 min (KBr): full-range (A) and expanded (B) spectra.

Additionally, the formation of poly(DBF) was not confirmed by size-exclusion chromatography (SEC) (**Figure 2.3**), confirming that the reaction is clean.

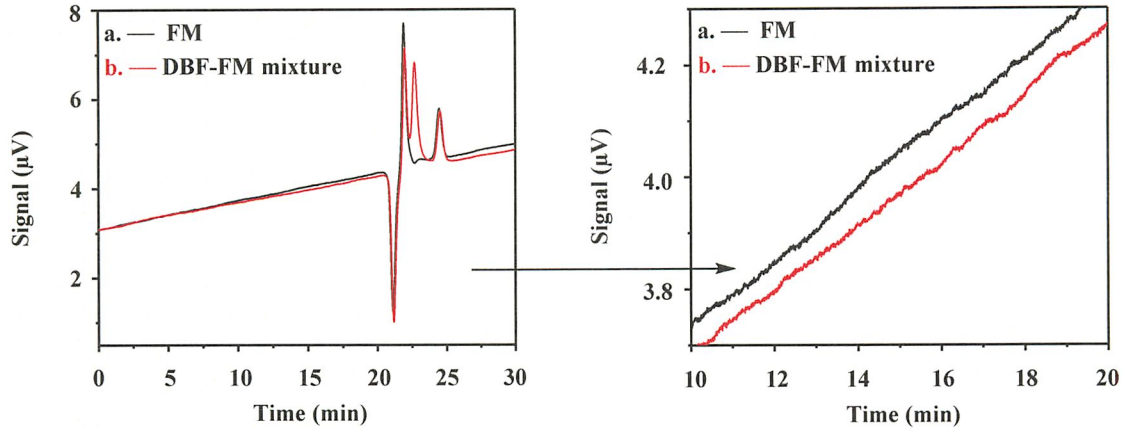

Figure 2.3. SEC profiles of FM (a) and a reaction mixture of FM containing DBF ($[FM]_0$ = 3.9 x 10^{-5} M, irradiation time = 70 min) (b): full-range (A) and expanded chromatograms (B).

In order to obtain information on the photochemical dehydration of FM, kinetic analyses were conducted on reactions carried out under various conditions, i.e., at different concentrations in hexane, in the presence and absence of a radical scavenger and in different solvents (hexane, acetonitrile, methanol, and H_2O) **(Figure 2.4 and Table 2.1)**. The amount of DBF generated by the reaction was quantified on the basis of the intensity of the UV signal at 256 nm corresponding to DBF **(Figure 2.5).**

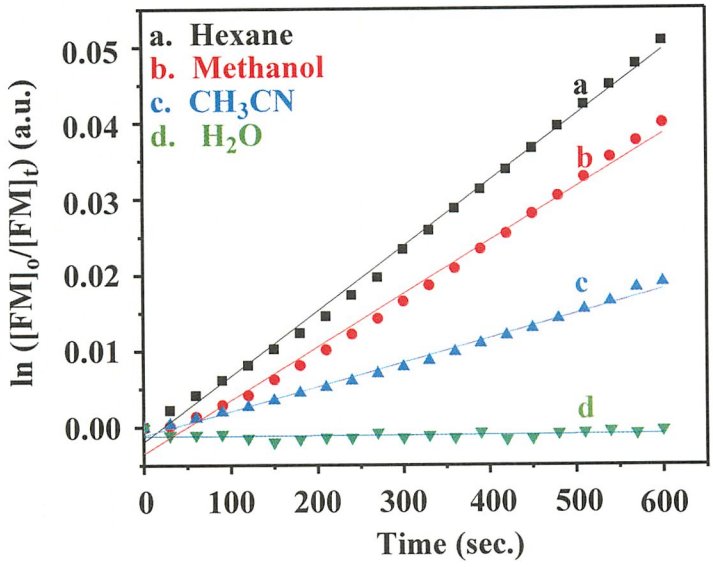

Figure 2.4. First-order rate plots for DBF production from FM upon irradiation in hexane ($[FM]_0 = 3.9 \times 10^{-5}$ M) (a), acetonitrile ($[FM]_0 = 3.9 \times 10^{-5}$ M) (b), methanol ($[FM]_0 = 4 \times 10^{-5}$ M) (c), and H_2O ($[FM]_0 = 3.9 \times 10^{-5}$ M) (d).

Table 2.1. First-order rate constants for DBF production from FM upon irradiation in hexane under various conditions at 23 °C[a]

Run	Solvent	FM (M)	k^b (sec^{-1})	ε^c	Φ^d
1	Hexane	3.9×10^{-5}	8.6×10^{-5}	1.89	0.12
2[e]	Hexane	3.9×10^{-5}	8.5×10^{-5}		
3	MeOH	4×10^{-5}	7×10^{-5}	33.62	0.29
4	CH_3CN	3.9×10^{-5}	3.2×10^{-5}	37.50	0.35
5	H_2O	3.9×10^{-5}	~0[f]	80.37	0.33

[a] Irradiation using a 300 W Xe lamp. [b] Determined at a conversion of 5.0% or lower by UV spectroscopy. [c] Dielectric constant data cited from ref. 12 . [d] Determined using 9,10-diphenylanthracene as a standard compound (F = 0.90, ref. 13). [e] In the presence of 2,2,6,6-tetramethyl4-piperidinol (5.1×10^{-4} M). [f] No products were detected.

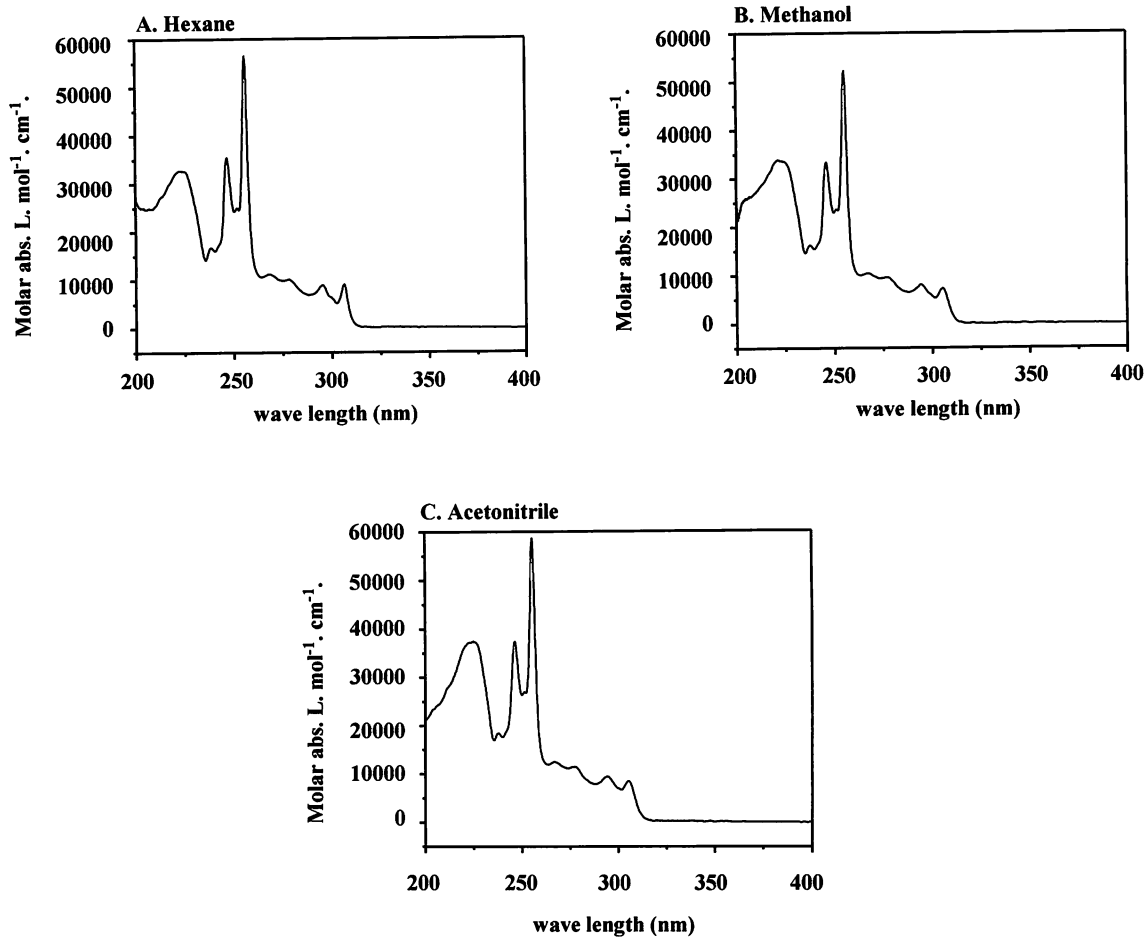

Figure 2.5. Absorbance spectra of FM in hexane (1.99 x 10^{-5} M) (A), methanol (2.06 x 10^{-5} M) (B), and acetonitrile (1.70 x 10^{-5} M) (C) in different solvents (cell path length = 1 cm; temp. = 23 °C).

Table 2.2. Molar absorptivities of DBF in various solvents[a]

Solvent	$\lambda_1$max	ε_1	$\lambda_2$max	ε_2	$\lambda_3$max	ε_3	$\lambda_4$max	ε_4
Hexane	306.2	9080	295.4	8930	278.0	10100	268.0	11200
Methanol	305.4	7220	294.4	8040	276.8	9530	266.8	10400
Acetonitrile	305.4	8440	294.4	9420	277.0	11400	266.6	12400

Solvent	$\lambda_5$max	ε_5	$\lambda_6$max	ε_6	$\lambda_7$max	ε_7	$\lambda_8$max	ε_8
Hexane	256.0	56500	251.8	25000	246.8	35500	224.0	32700
Methanol	255.4	52300	251.4	23600	246.2	33400	221.4	33900
Acetonitrile	255.4	58700	251.4	26900	246.4	37400	225.0	37500

[a]Minimum wavelength resolution setting = 0.2 nm.

First, the dependence of the initial reaction rate on the concentration of FM was examined in hexane at $[FM]_0$ = 7.5 x 10^{-5} M, 5.0 x 10^{-5} M, 3.9 x 10^{-5} M, 1.5 x 10^{-5} M and 1.0 x 10^{-5} M (**Figure 2.6**) for 600 s duration of the reaction (conversion < 5.0%); the reaction was found to be almost first order with respect to $[FM]_0$, where the slope was 1.06. This result suggests that the photo-induced β-elimination of FM is an almost unimolecular reaction.

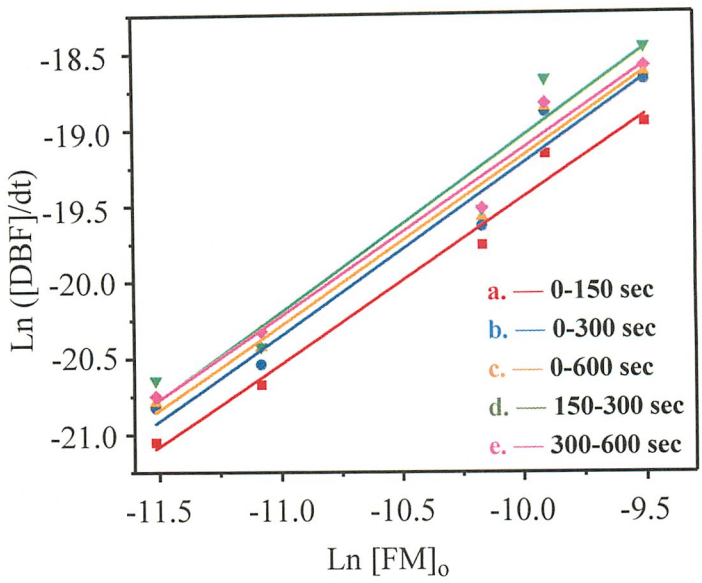

Figure 2.6. Conc. vs. initial reaction rate plots of photo-generated DBF in hexane at [FM]o = 7.5 x 10^{-5} M, 5.0 x 10^{-5} M, 3.9 x 10^{-5} M, 1.5 x 10^{-5} M, and 1.0 x 10^{-5} M for different durations of reaction. The data have been normalized to match the results reported in **Table 2.1 and Figure 2.4** at [FM]o = 3.9 x 10^{-5} M in order to minimize errors due to aging of the Xe lamp.

Figure 2.4 indicates the first-order plots of the reactions in different solvents. All the reactions at low conversions (< 5.0%) exhibited almost linear relations according the following equation:

$$Ln\left(\frac{[FM]o}{[FM]t}\right) = kt$$

where $[FM]_0$ and $[FM]_t$ are the concentrations of FM before starting irradiation and at a given duration of irradiation (t), respectively, k is the first-order rate constant, and t is the duration of irradiation. The data points in all the reaction plots in this work were well approximated by linear lines, and the first-order rate constant (k) values were determined in the range of conversion of 0-5.0% **(Table 2.1)**.

The solvent remarkably affected the reaction rate; the rate constants decreased in the following order of solvents, i.e., in hexane, in MeOH, in CH_3CN, and in H_2O **(Figure 2.4 and Table 2.1)**. The order of the solvents seems to be in accordance with the order of their dielectric constants (ε). The solvent polarity effect is opposite to that expected from the deprotonation-based mechanism in the ground state;[11] a polar reaction involving deprotonation would be faster in a solvent with a higher dielectric constant. The reaction therefore may not go through an E1cb mechanism involving a raw carbanion at the 9-position of the fluorene backbone. The reaction in excited states may proceed rather through a mechanism which is not mediated by an ionic species.

In regard of these experiments in different solvents, it was confirmed that the absorbance of FM had a linear relationship with the concentration in the range of concentration discussed in this work **(Figure 2.7 and Figure 2.8)**. This result strongly suggests that FM is molecularly dispersed without aggregate formation in all solvents including H_2O.

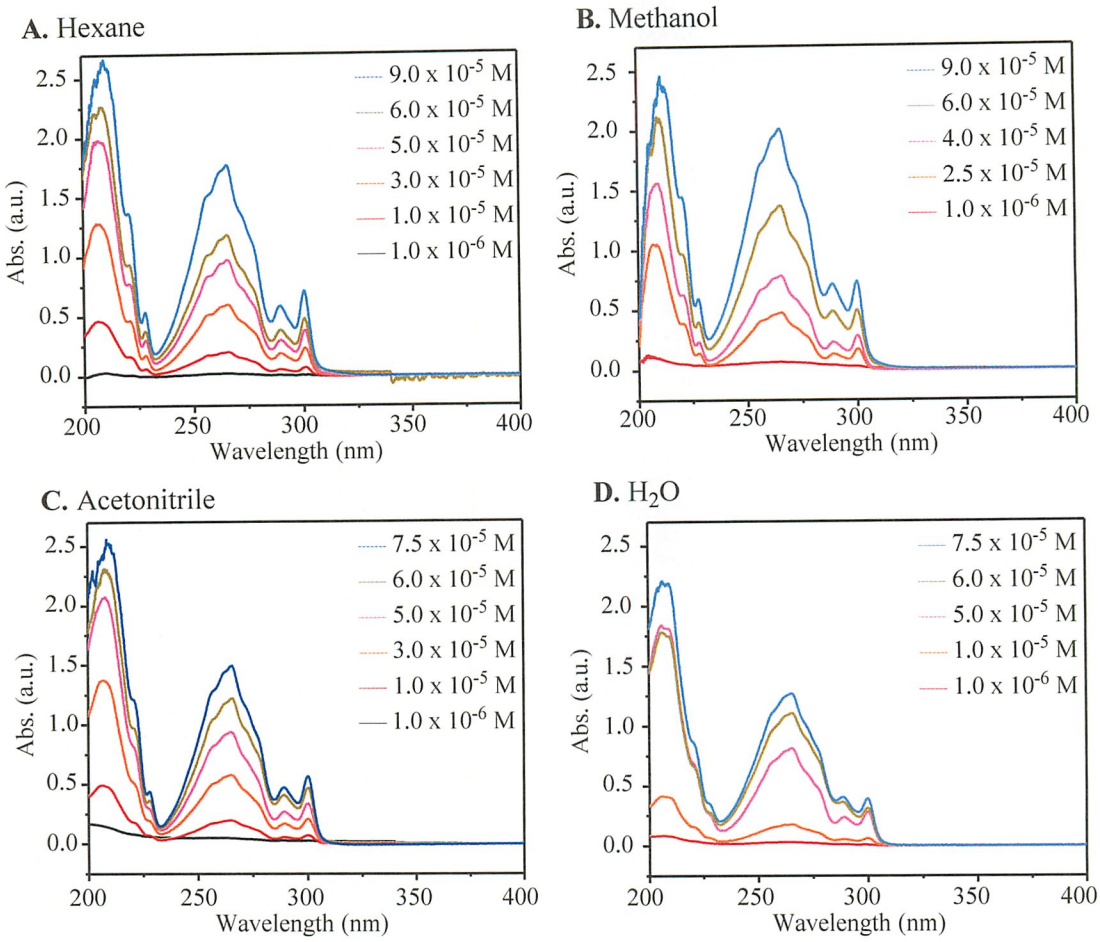

Figure 2.7. Absorbance spectra of FM in hexane (A), methanol (B), acetonitrile (C), and H_2O (D) at different concentrations (cell path length = 1 cm; temp. = 23 °C).

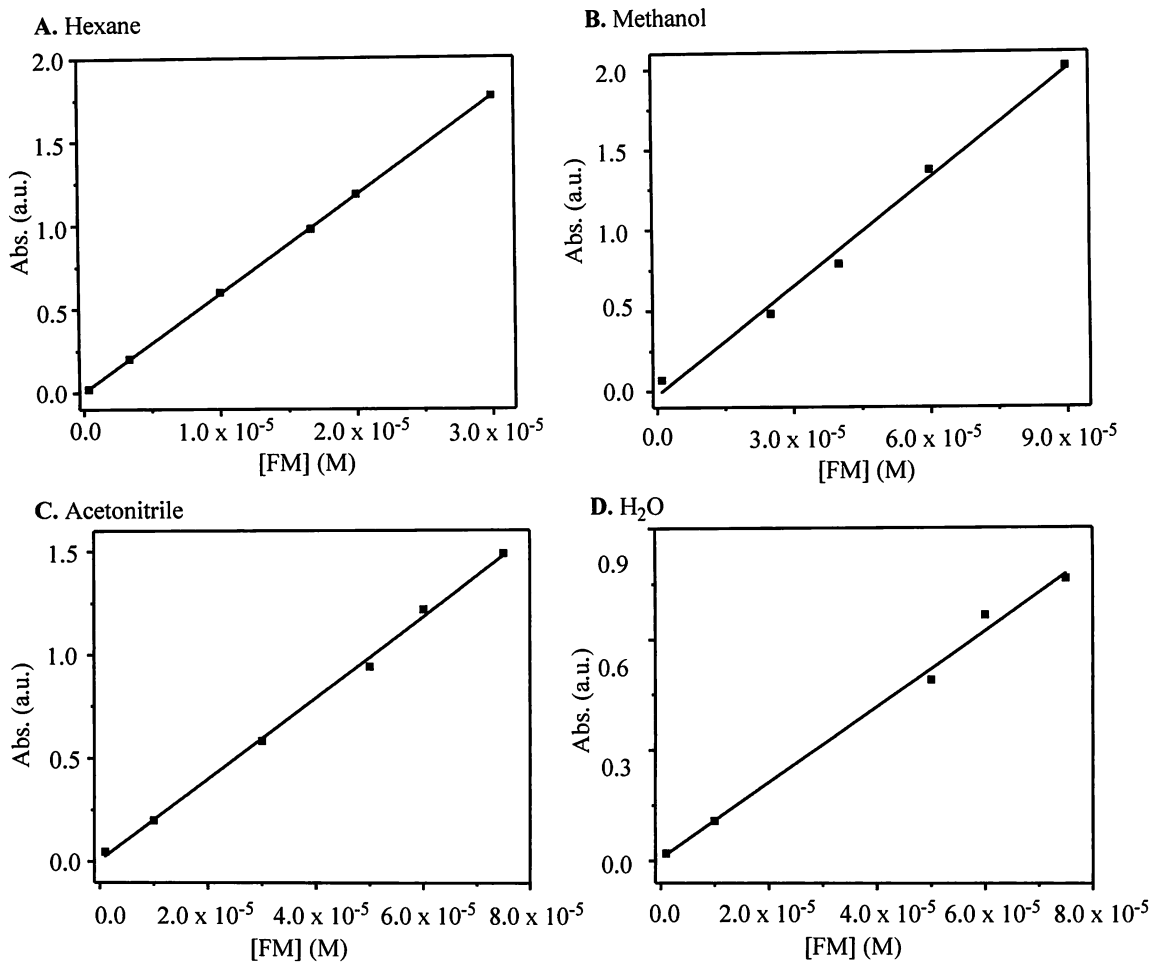

Figure 2.8. Absorbance-vs.-concentration plots for FM in hexane (A), methanol (B), acetonitrile (C), and H_2O (D) (cell path length = 1 cm; temp. = 23 °C).

In addition, as far as the organic solvents are concerned, the rate constant was higher in a solvent in which the fluorescence efficiency (Φ) of FM was lower. This result may be in line with an assumption that the reaction would occur through a triplet excited state similarly to many other photo chemical reactions. A lower fluorescence quantum yield may be caused in part by a higher efficiency of intersystem crossing leading to a higher chance of generating a triple-state active species (quenching by the reaction) although

efficient non-radiative deactivation to the ground state directly from singlet excited states may also contribute.

Additionally, the molar absorptivity of FM was rather smaller in acetonitrile and in H_2O than in hexane and in MeOH **(Table 2.3)** (hypochromicity) which may be suggestive of π-stacking interactions between FM molecules in the ground state.

Table 2.3. Molar absorptivies of FM in various solvents.

Solvent	λ_{max} (nm)	ε (L mol^{-1} cm^{-1})
Hexane	265.8	20000
Methanol	265.5	24700
Acetonitrile	265.0	18400
H_2O	265.2	16000

However, the emission spectral shape of FM with the emission maximum wavelength of 304 nm was unchanged without any new signals based on excimer formation upon changing the solvent (**Figure 2.9**) These results suggest that π -stacking interactions in the ground state, if any, may be too weak to promote excimer interactions in excited states which could affect the reaction rate.

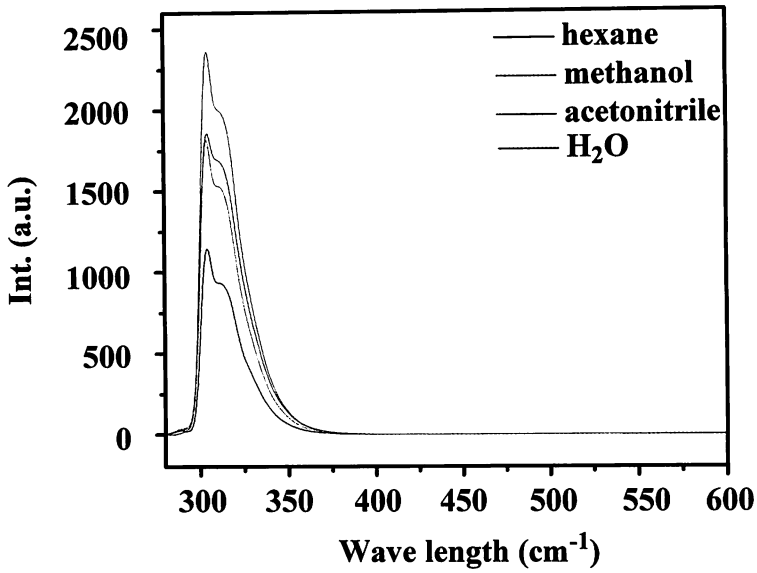

Figure 2.9. Emission spectra of FM in various solvents (excitation wavelength = 265 nm; cell path length = 1 cm).

Table 2.4. The Fluorescence analysis of FM in hexane, methanol, acetonitrile, and H_2O at 23 °C[a]

Run	Solvent	λ_{max1} (nm)	Intensity (a.u.)	Φ^b
1	hexane	304.2	1143.39	0.12
2	methanol	304.2	1815.95	0.29
3	acetonitrile	304.6	2362.57	0.35
4	H_2O	304.6	1855.03	0.33

[a][FM] = 1.0 x 10^{-6} M, λ_{ex} = 265 nm. [b]Determined using 9-10-diphenylanthracene as a standard compound (F = 0.90).

Further, the presence of 2,2,6,6-tetramethyl-4-pieridinol, a radical scavenger, had little effect on the reaction in hexane **(runs 1 and 2 in Table 2.1)**. In addition, the presence of oxygen contained in air did not significantly affect the reaction **(Figure 2.10)**. These results suggest that the reaction system does not involve free-radical species.

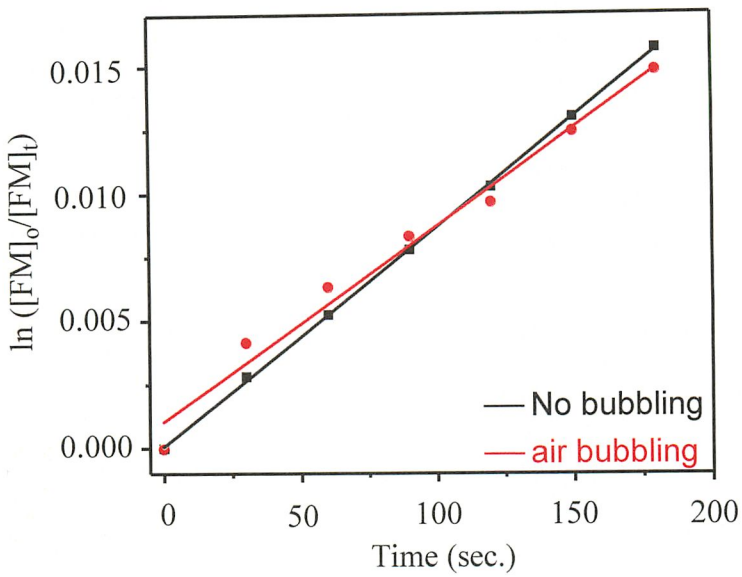

Figure 2.10. First-order rate plots for DBF production from FM on irradiation in hexane distilled under N_2 (A) and in hexane bubbled with air (B) ($[FM]_0 = 3.9 \times 10^{-5}$ M) . The latter solution was bubbled for 10 min before starting the reaction, and further bubbled for 1 min after each spectral measurement. The data have been normalized to match the results reported in **Table 2.1 and Figure 2.4** at $[FM]_0 = 3.9 \times 10^{-5}$ M in order to minimize errors due to aging of the Xe lamp.

In order to shed light on the reaction mechanism, density function theory (DFT) calculations were conducted on the transformation of FM **(Figure 2.11)**. Some of the transition states were obtained using the GRRM package.[14] The black, purple, and red paths correspond to those in the S_0, S_1, and T_1 states, respectively. When photoexcited from the S_0 state to the S_1 state followed by structural relaxation, the conformation of FM slightly changes mainly through the rotation around the single bond connection of the 9-poisiton carbon and the -CH_2- group (S_1-min). FM then proceeds to the key transition state in the triplet state (T_1-TS1) involving homolysis of the CH_2-O bond leading to an OH radical and an 9-fluorenylmethyl radical. The OH radical appears to interact with the hydrogen at the 1-position of the fluorene backbone possibly through

weak hydrogen-bonding (T_1-IM1 and T_1-IM2) before it interacts with the hydrogen at the 9-position in the second transition state (T_1-TS2) which leads to abstraction of the hydrogen leading to DBF (T_1-IM3). The methylene unit in DBF is perpendicular to the fluorene backbone in the triplet state (T_1-IM3) and becomes coplanar when it is deactivated to the S_0 state via the minimum energy intersystem crossing point (MEISCP).

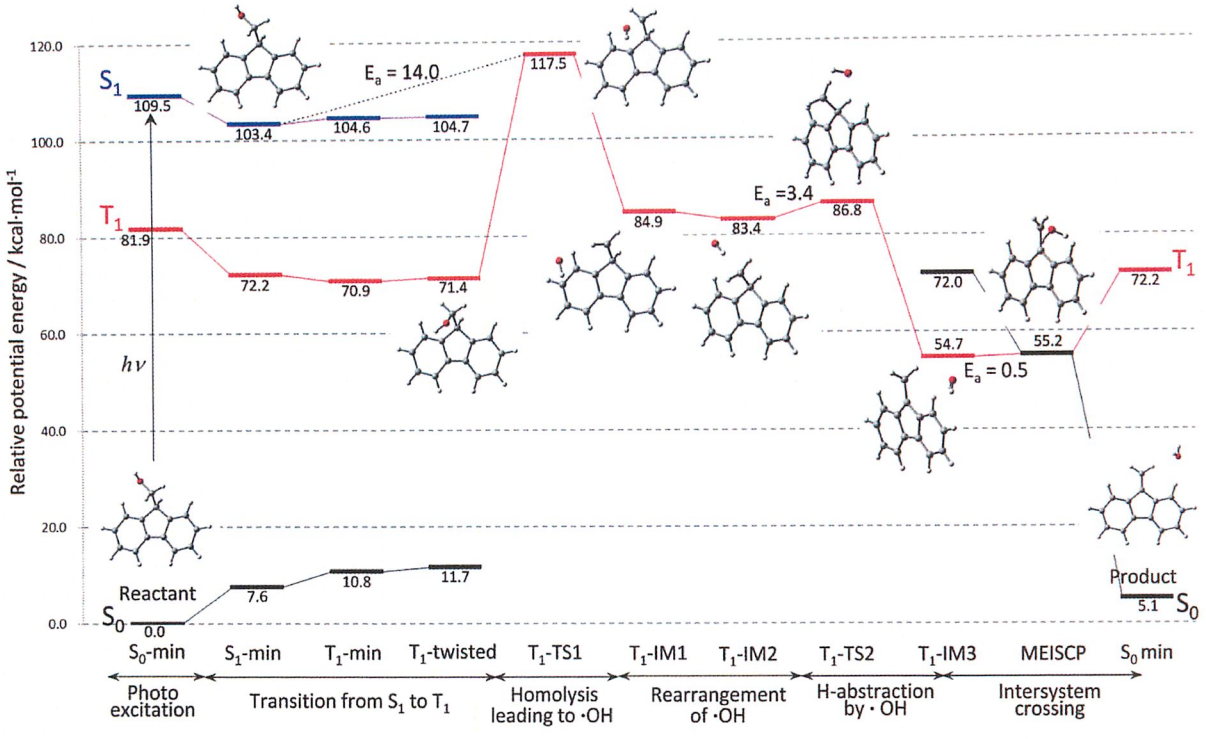

Figure 2.11. Proposed mechanism of the photo-induced β-elimination of 9-fluorenylmethanol leading to dibenzofulvene. Numbers and E_a denote relative potential energies and activation energy in kcal mol^{-1}, respectively. MEISCP stands for the minimum energy intersystem crossing point.

The β-elimination is thus expected to occur through a concerted mechanism where radical species have a role. Although the reaction in the presence of a radical scavenger

did not affect the rate constant **(run 2 in Table 2.1)**, the life times of the proposed OH and 9-fluorenylmethyl radicals may be too short in the concerted reaction that the two species cannot collide with the scavenger or oxygen. The nature of the proposed radical species may be different from that of general free-radical species.

In connection to the proposed mechanism, the polar solvent effects discussed earlier may be interpreted in terms of mobility of the reactive species. The OH radical may be interacted with MeOH or CH_3CN or H_2O through hydrogen-bonding and/or dipole-dipole interactions, and therefore have lower mobility in polar solvents than in hexane leading to less efficiency in the rearrangements (T_1-IM1 and T_1-IM2), depicted in **(Figure 2.11).**

The mechanism predicted by the DFT calculations is in a sharp contrast to the facts that fluorene derivatives[15,16] and benzylalcohol derivatives[17] have been expected to form an ion or radical on the carbon atom at the benzylic position where the active species can be stabilized by conjugation with the aromatic system. Homolysis of the CH_2-O bond of FM is hence unexpected. As DFT methods have been used to successfully interpret radical reactions,[18,19] we believe that the predicted radial mechanism can be trusted.

2.4 Conclusion

We disclosed the first photo-induced β-elimination reaction through a radical-mediated mechanism leading to a useful olefin compound. The observed effects of solvents and additives and the results of theoretical calculations suggested that the radical species may have a role in the olefin formation. Although the scope of the photo-induced β-elimination reaction is still limited to the conversion of 9-fluorenylmethanol so far, the scope of the substrate may be expanded through future research work.

2.5 References

1 (a) N. J. Turro, Modern molecular photochemistry, University science books, U.S.A., 1991; (b) Handbook of photochemistry, ed. M. Montalti, A. Credi, L. Prodi and M. T. Gandolfi, CRC Press, Boca Raton, 3rd edn, 2006; (c) Synthetic organic photochemistry, ed. A. G. Griesbeck and J. Mattay, CRC Press, New York, 2004; (d) N. J. Turro, V. Ramamurthy and J. C. Scaiano, Principles of molecular photochemistry: an introduction, University science books, U.S.A., 2009; (e) D. Cowan and R. L. Drisko, Elements of organic photochemistry, Springer Science & Business Media, New York, 2012; (f) G. Geoggroy and M. S. Wrighton, Organometallic photochemistry, Elsevier, New York, 2012; (g) D. M. Roundhill, in Photochemistry and photophysics of metal complexes, ed. P. John and J. Fackler, Springer Science & Business Media, New York, 1994.

2 H. Uno, Y. Naruta and K.Maruyama, Syntheses of (±)-aklavinones : Application of the stereocontrolled "zipper" bicyclo cyclization reaction, Tetrahedron, 1984, **40**, 4725–4741.

3 B. E. Maryanoff and A. B. Reitz, The Wittig olefination reaction and modifications involving phosphoryl-stabilized carbanions. Stereochemistry, mechanism, and selected synthetic aspects, Chem. Rev., 1989, **89**, 863–927.

4 N. A. Petasis and E. I. Bzowej, Titanium-mediated carbonyl olefinations. 1. Methylenations of carbonyl compounds with dimethyltitanocene, J. Am. Chem. Soc., 1990, **112**, 6392–6394.

5 D. J. Ager, The Peterson Reaction, Synthesis, 1984, 384–398.

6 D. W. Roberts and D. L. Williams, Sultone chemistry, Tetrahedron, 1987, **43**, 1027–1062.

7 J. E. McMurry, Carbonyl-coupling reactions using low-valent titanium, Chem. Rev., 1989, **89**, 1513–1524.

8 R. H. Shapiro, Alkenes from Tosylhydrazones, Org. React., 1976, **23**, 405–507.

9 S. Hosokawa and M. Isobe, Reductive decomplexation of biscobalthexacarbonyl acetylenes into olefins, Tetrahedron Lett., 1998, **39**, 2609–2612.

10 (a) T. Nakano, K. Takewaki, T. Yade and Y. Okamoto, Dibenzofulvene, a 1,1-Diphenylethylene Analogue, Gives a π-Stacked Polymer by Anionic, Free-Radical, and Cationic Catalysts, J. Am. Chem. Soc., 2001, **123**, 9182–9183; (b) T. Nakano and T. Yade, Synthesis, Structure, and Photophysical and Electrochemical Properties of a π-Stacked Polymer, J. Am. Chem. Soc., 2003, **125**, 15474–15484; (c) T. Nakano, O. Nakagawa, M. Tsuji, M. Tanikawa, T. Yade and Y. Okamoto, Poly(2,7-di-*n*-pentyldibenzofulvene) showing chiroptical properties in the solid state based purely on a chiral conformation, Chem. Commun., 2004, 144–145; (d) T. Nakano, T. Yade, Y. Fukuda, T. Yamaguchi and S. Okumura, Free-Radical Polymerization of Dibenzofulvene Leading to a π-Stacked Polymer: Structure and Properties of the Polymer and Proposed Reaction Mechanism, Macromolecules, 2005, **38**, 8140–8148; (e) T. Nakano, O. Nakagawa, T. Yade and Y. Okamoto, Solid-State Polymerization of Dibenzofulvene Leading to a Copolymer with Oxygen, Macromolecules, 2003, **36**, 1433–1435; (f) T. Nakano, T. Yade, M. Yokoyama and N. Nagayama, Charge Transport in a π-Stacked Poly(dibenzofulvene) Film, Chem. Lett., 2004, **33**, 296–297; (g) T. Nakano, Synthesis, structure and function of π-stacked polymers, Polym. J., 2010, **42**, 103–123.

11 (a) R. M. O'Ferrall and S. J. Slae, The Reaction of 9-Fluorenylmethanol with Base: a Carbanion Mechanism of β- Elimination, J. Chem. Soc. D, 1969, 486–487; (b) R. M. O'Ferrall and S. J. Slae, β-Elimination of 9-fluorenylmethanol in aqueous solution: an E1cB mechanism, J. Chem. Soc. B, 1970, 260–268; (c) R. M. O'Ferrall, β-Elimination of 9-Fluorenylmethanol in Solutions of Methanol and t-Butyl Alcohol, J. Chem. Soc. B, 1970, 268–274.

12 (a) H. Schlundt, On the dielectric constants of pure solvents, J. Phys. Chem., 1901, **5**, 503–526; (b) A. A. Maryott and E. R. Smith, Table of dielectric constants of pure liquids, National Bureau of Standards circular, U.S. Govt. Print. Off., 1951, vol. 514, pp. 1–41.

13 (a) S. Hamai and F. Hirayama, Actinometric Determination of Absolute Fluorescence Quantum Yields, J. Phys. Chem., 1983, **87**, 83–89; (b) W. H. Melhuish, Quantum Efficiencies of Fluorescence of Organic substances: Effect of Solvent and Concentration of the Fluorescent Solute[1], J. Phys. Chem., 1961, **65**, 229–235.

14 (a) S. Maeda, Y. Harabuchi, Y. Osada, T. Taketsugu and K. Morokuma, see http://grrm.chem.tohoku.ac.jp/GRRM/ (as of April 22, 2017); (b) S. Maeda, K. Ohno and K. Morokuma, Systematic Exploration of the Mechanism of Chemical Reactions: The Global Reaction Route Mapping (GRRM) Strategy Using the ADDF and AFIR Methods, Phys. Chem. Chem. Phys., 2013, **15**, 3683–3701.

15 (a) E. V. Donckt, J. Nasielski and P. Thiry, Photochemistry of fluorene derivatives, J. Chem. Soc. D, 1969, 1249–1250; (b) J. F. Ireland and P. A. H. Wyatt, Acid-Base Properties of Electronically Excited States of Organic Molecules, Adv. Phys. Org. Chem., 1976, **12**, 131–159; (c) L. M. Tolbert, in Comprehensive Carbanion Chemistry, ed. E. Buncel and T. Durst, Elsevier, Amsterdam, 1987, part C.

16 (a) D. Budac and P. Wan, Excited-state carbon acids. Facile benzylic carbon-hydrogen bond heterolysis of suberene on photolysis in aqueous solution: a photogenerated cyclically conjugated eight π-electron carbanion, J. Org. Chem., 1992, **57**, 887–894; (b) E. Krogh and P. Wan, Contrasting photosolvolytic reactivities of 9-fluorenol vs. 5-suberenol derivatives. Enhanced rate of formation of cyclically conjugated four .pi. carbocations in the excited state, J. Am. Chem. Soc., 1989, **111**, 4887–4895; (c) H. Tomioka, H. Nakamura and Y. Izawa, Irradiation of diazofluorene in alcohols: unusual behaviour of fluorenyl ethers, J. Chem. Soc., Chem. Commun., 1983, 1070–1071.

17 P. Wan, Acid-catalyzed photochemical generation of benzyl cations as a probe of the electron-donating abilities of benzene substituents in the singlet excited state, J. Org. Chem., 1985, **50**, 2583–2586.

18 J. Aguilera-Iparraguirre, H. J. Curran, W. Klopper and J. M. Simmie, Accurate Benchmark Calculation of the Reaction Barrier Height for Hydrogen Abstraction by the Hydroperoxyl Radical from Methane. Implications for C_nH_{2n+2} where n = 2 → 4 Jorge, J. Phys. Chem. A, 2008, **112**, 7047–7054.

19 O. Tishchenko and D. G. Truhlar, Benchmark Ab Initio Calculations of the Barrier Height and Transition-State Geometry for Hydrogen Abstraction from a Phenolic Antioxidant by a Peroxy Radical and Its Use to Assess the Performance of Density Functionals, J. Phys. Chem. Lett., 2012, **3**, 2834–2839.

Chapter 3

Cationic polymerization of dibenzofulvene leading to a π-stacked polymer

3.1. Introduction

Polymer chain conformation often affects the properties and function of polymeric materials; conformational control through polymerization is thus important. Representative macromolecules with controlled chain conformation include helical and π-stacked polymers. [1-5] π-Stacked conformations can be found in polymers including poly(dibenzofulvene) (poly(DBF)) and derivatives,[6-9] polyether,[10] polyurethane,[11] polyphanathroline,[12] polyketone,[13] poly(benzofulvene) and derivatives,[14-15] and those based on cyclophanes.[16-19] Poly(DBF) is the first vinyl polymer having a π-stacked conformation in which the main-chain C-C bonds are nearly all trans and the side-chain fluorene moieties are stacked on top of each other **(Scheme 3.1)**.[6,7] Such a conformation was fully elucidated by spectroscopic and x-ray crystallographic analyses of isolated oligomers having defined chain lengths. Poly(DBF) exhibits intriguing photo electronic properties including a high charge mobility for a vinyl polymer ($\mu = 2.7 \times 10^{-4}$ $cm^2\ V^{-1}s^{-1}$ at 299 K at $F = 7 \times 10^5$ V/cm) which is higher than those of some main-chain conjugating polymers such as poly(*p*-phenylenevinylene) (1×10^{-5} $cm^2\ V^{-1}\ s^{-1}$) and poly(methylphenylsilane) (1×10^{-4} $cm^2\ V^{-1}s^{-1}$) due to its strictly controlled π-stacked chain conformation.[20]

This polymer can be prepared by ionic or radical polymerization of DBF and full details of anionic and radical polymerization have been explored[6,21] while cationic polymerization has not yet been extensively studied. Herein we report the detailed results of cationic polymerization of DBF with an emphasis on the stereochemistry of polymerization **(Scheme 3.1)**. In general, among various addition polymerization techniques, anionic polymerization and coordination polymerization have been mostly

applied for the synthesis of stereo-controlled polymers of a wide variety of chemical structure, and there also have been examples of successful stereo regulation by radical polymerization of monomers leading polymers with a rigid conformation and polar monomers in the presence of Lewis acids. In a sharp contrast, achievements in stereo regulation by cationic polymerization have been much less significant compared with those by the other techniques. In this context, stereochemical studies on cationic polymerization of DBF which is expected to lead to a rigid, π-stacked conformation of resulting polymer may open a new phase of cationic polymerization chemistry.

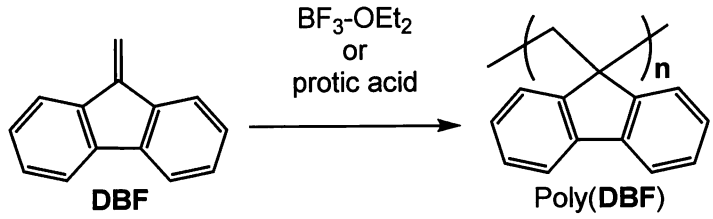

Scheme 3.1. Cationic polymerization of DBF.

3.2 Experimental

3.2.1 Materials

DBF was prepared according to the literature.[6,7] BF_3-OEt_2 (95%, Kanto), CH_3CO_2H (TCI), CF_3CO_2H (TCI), were CH_3SO_3H (TCI) were used as obtained. Styrene (TCI) and CH_2Cl_2 were dried and distilled over CaH_2.

3.2.2 Instrumentation

NMR spectra were recorded on a JEOL JMN-ECX400 spectrometer. Size-exclusion chromatography (SEC) measurements were carried out using a chromatographic system consisting of a JASCO DG-980-50 degasser, a HITACHI L-7100 pump, a HITACHI L-7420 UV-Vis detector and a HITACHI L-7490 RI detector, equipped with TOSOH TSKgel G3000H HR and G6000H HR columns (30 × 0.72 (i.d.) cm) connected in series

(eluent: THF, flow rate: 1.0 mL/min). Preparative recycling SEC was performed with a JAI LC-9201 chromatograph consisting of a JAI PI-50 pump and a Soma S-3740 UV/Vis detector equipped with JAIGEL 1H and 2H columns (60 × 2 (i.d.) cm) connected in series (eluent: $CHCl_3$, rate: 3.5 mL/min). UV-Vis spectra were taken using quartz cells on JASCO V-550 and V-570 spectrophotometers, and fluorescence spectra were measured using quartz cells on a JASCO PF-8500 fluorescence spectrophotometer. MALDI-TOF mass spectra were collected on a Bruker UltraFlex III and autoflex machine using dithranol (DIT) as matrix. 10.0 mg DIT dissolved in 1.0 mL THF.

3.2.3 Polymerization

Typical procedure of polymerization **(entry 3 in Table 3.1)**: DBF (178 mg, 1.00 mmol) was dissolved in 5 ml of CH_2Cl_2 under N_2 atmosphere in a 10-ml round bottomed flask sealed with a three-way stop cock. A BF_3-OEt_2 solution in CH_2Cl_2 (0.775 M) (261 μl, 0.202 mmol) was added with a hypodermic syringe to the monomer solution cooled at 0 °C, and the reaction was run for 24 h. After confirming the monomer conversion ratio by NMR analysis of an aliquot of the mixture, the reaction mixture was poured into a large excess of MeOH, and the MeOH-insoluble part was collected with a centrifuge. The MeOH-insoluble part was further separated into THF-soluble and insoluble parts through reprecipitation and collection with a centrifuge.

3.3. Results and Discussion

3.3.1. Polymerization behavior

Cationic polymerization of DBF was conducted in CH_2Cl_2 using BF_3-OEt_2 as catalyst at -40°C, 0°C, and 40°C or using CH_3CO_2H, CF_3CO_2H, or CH_3SO_3H as initiator at 0°C at various monomer and catalyst concentrations. The conditions and results are summarized in **Table 3.1**. In the polymerization using BF_3-OEt_2 under all conditions at $[DBF]_0$ = 0.2 M and 0.1 M at 0°C, the monomer was almost completely consumed

while the monomer conversion ratio was lower at $[DBF]_o$ = 0.05 and 0.025 M. As we previously reported, the anionic and radical polymerization products of DBF contained significant amounts of insoluble polymers. The insolubility of the polymer is considered to arise from close packing of chains with the controlled conformation. In addition, the yield of insoluble polymer is known to be higher at a condition where the production of a longer chain is expected. The cationic polymerization products were also mostly insoluble in solvents, suggesting that the cationic polymerization products possess a controlled conformation.

In more detail, the yield of THF-insoluble polymer tended to be higher at a higher $[DBF]_o$ at a constant $[DBF]/[BF_3]$ ratio ($[C/I]_o$ in **Table 3.1**) of 5 **(runs 3, 6, 7, and 8 in Table 3.1)**. On the other hand, $[DBF]/[BF_3]$ ratio seemed not to clearly affect the yield of THF-insoluble polymer at a constant $[DBF]_o$ of 0.2 M. These results indicate that DBF concentration is an important controlling factor of chain length in the cationic polymerization while [monomer]/[initiator] ratio is not.

Temperature effects can be read from **runs 3, 9, and 10 in Table 3.1** at $[DBF]_o$ = 0.2 M and $[BF_3]_o$ = 0.04 M. While the monomer was almost completely consumed under these three conditions, the yield of THF-insoluble product at 40°C was obviously lower than those at -40°C and 0°C. These results might suggest that chain transfer may have more significant role at 40°C than at 0°C and -40°C.

In addition, it is noteworthy that CH_3SO_3H effectively polymerized DBF **(runs 11 and 12 in Table 3.1)**. The monomer was almost completely consumed in the systems with CH_3SO_3H at 0°C while this initiator leads to much lower monomer conversions (3-4 %) in the polymerization of styrene under the same conditions. DBF was also polymerized using CF_3CO_2H and CH_3CO_2H **(runs 13 and 14 in Table 3.1)** while these initiators were not effective for styrene polymerization under the same conditions. These results clearly indicate that DBF is a highly reactive monomer in cationic polymerization as well as in anionic and radical polymerizations.

The monomer conversion in the polymerizations using the protonic acids at 0°C **(runs 11, 13, 14 in Table 3.1)** at $[DBF]_o$ = 0.2 M and $[acid]_o$ = 0.04 M seems to increase with a decrease in pKa of the acids, i.e., 1.6 for CH_3SO_3H, 3.4 for CF_3CO_2H, and 12.3 for CH_3CO_2H (in DMSO),[22,23] supporting that proton is the initiating species. It is interesting that CF_3CO_2H and CH_3CO_2H having largely different pKa's led to rather similar monomer conversions. Some interaction between DBF molecules and the acid molecules or the corresponding counter anions may have a role in the polymerization behaviors with the three acids.

Table 3.1. Cationic polymerization of DBF in CH_2Cl_2 for 24 h[a]

Run	C/I[b]	Temp. [°C]	$[DBF]_o$ [M]	$[C/I^{b)}]_o$ [M]	Conv.[c] [%]	MeOH-insoluble product			
						THF-Insol.	THF-sol.		
						Yield [%]	Yield [%]	$Mn^{d)}$ (vs PSt)	$Mn^{e)}$ (vs DBF)
1	BF_3-OEt_2	0	0.2	0.2	>99	90	9[f]	340	490
2	BF_3-OEt_2	0	0.2	0.1	>99	96	3[f]	370	520
3	BF_3-OEt_2	0	0.2	0.04	>99	95	4[f]	320	460
4	BF_3-OEt_2	0	0.2	0.02	>99	98	1[f]	320	460
5	BF_3-OEt_2	0	0.2	0.01	>99	96	3[f]	300	430
6	BF_3-OEt_2	0	0.1	0.02	>99	78	9	640	920
7	BF_3-OEt_2	0	0.05	0.01	89	68	8	690	990
8	BF_3-OEt_2	0	0.025	0.005	63	56	7[f]	680	970
9	BF_3-OEt_2	40	0.2	0.04	>99	13	29	1010	1440
10	BF_3-OEt_2	-40	0.2	0.04	>99	74	11[f]	500	720
11	CH_3SO_3H	0	0.2	0.04	>99	80	4	590	840
12	CH_3SO_3H	0	0.05	0.01	>99	49	9	640	920
13	CF_3CO_2H	0	0.2	0.04	17	8	6	1640	2350
14	CH_3CO_2H	0	0.2	0.04	10	2	6	2250	3220

[a]DBF (178 mg, 1.00 mmol); [b]C/I denotes "catalyst or initiator"; [c]Determined on the basis of ^1H NMR analysis of crude products and the ratio of MeOH-insoluble, THF-insoluble part, MeOH-insoluble, THF-soluble part, and MeOH-soluble part; [d]Determined by SEC using polystyrene standards; [e]Mn value relative to poly(dibenzofulvene). Calculated by multiplying the Mn values relative to standard polystyrenes by a factor of 1.43 which was obtained through a comparison of ten experimental Mn values relative to standard polystyrene and those relative to standard poly(dibenzofulvene) reported in ref. 21. [f]Calculated on the basis of theoretical total polymer yields and experimental yields of THF-insoluble products.

Figure 3.1 indicates the IR spectra of insoluble poly(DBF)s prepared by cationic, anionic and radical polymerizations. Through a change in aromatic substitution that can occur through isomerization of the growing species may be reflected in IR spectra typically in the range of 2000-1750 cm^{-1}, the three spectra in **Figure 3.1** have very similar spectral patterns, indicating that the cationic polymerization does not involve isomerization of growing species as well as anionic and radical polymerization.

In addition, the polymers prepared using BF_3-OEt_2 and CH_3SO_3H exhibited signals of mass numbers of 875.4, 1055.6, 1233.6, 1411.8, 1589.8 and those of 875.5, 1055.6, 1233.708, 1410.8, 1589.9, respectively **(Figure 3.2)**. The spacing of the peaks is ca. 178-180 which is close the DBF unit molar mass. These results support that the polymers prepared by cationic polymerization have no chemical structural defects as well as those made by radical and cationic polymerization.

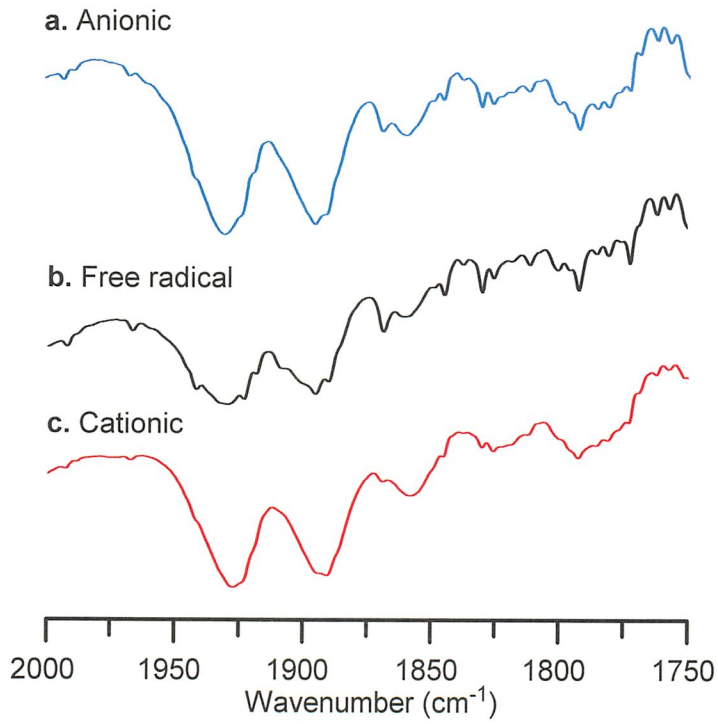

Figure 3.1. IR spectra of poly(DBF)s prepared by anionic (a), radical (b), and cationic (c) polymerizations. [THF-insoluble polymers, KBr pellet]

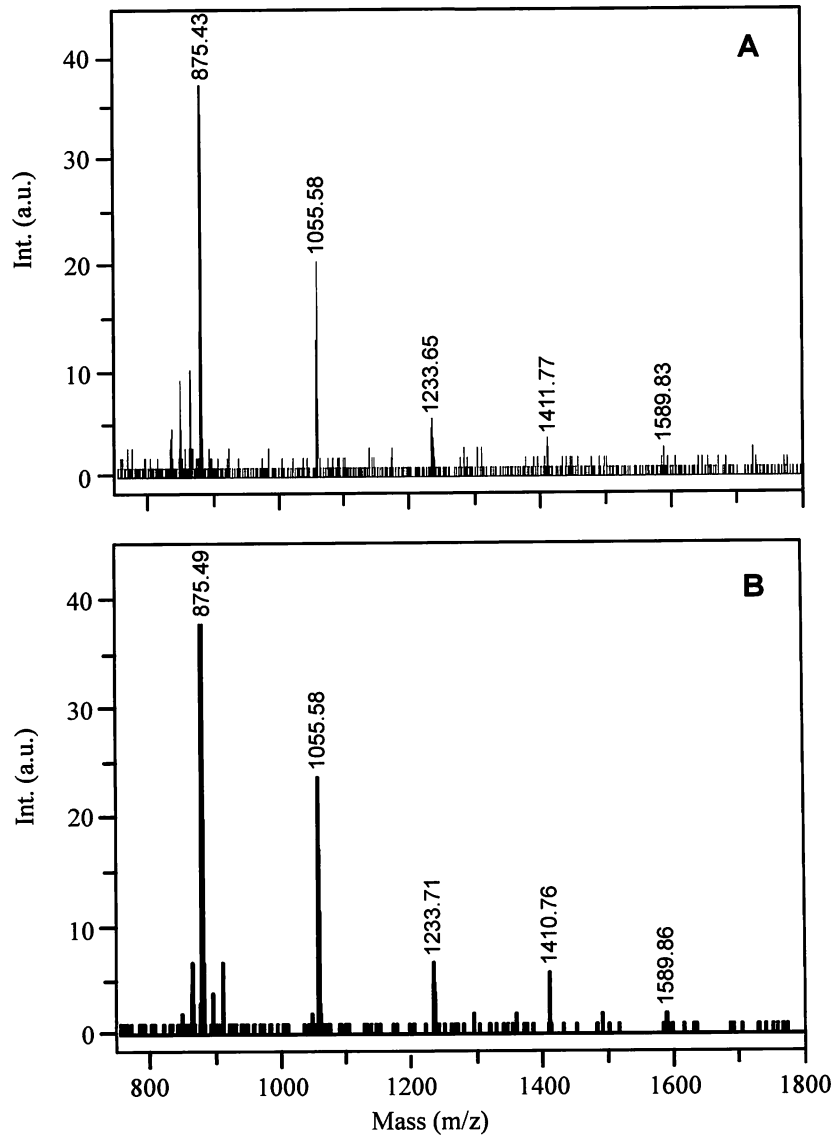

Figure 3.2. MALDI-TOF mass spectra of THF-soluble poly(DBF)s prepared using BF_3-OEt_2 **(run 10 in Table 3.1)** and (A) and using CH_3SO_3H **(run 11 in Table 3.1)** (B). Samples were prepared by depositing 1μL of poly(DBF) solution in $CHCl_3$ (7 mg/mL) onto pre-formed thin layer of dithranol matrix by drop-casting 1μL of THF solution (10 mg/mL, 4.42 x 10^{-2} M) in a sample well.

3.3.2. Chain conformation and polymer properties

Because poly(DBF) does not have any centers of chirality, chain conformation is the focus of stereochemical studies. Chain conformation of poly(DBF) prepared by cationic polymerization was assessed by ^1H NMR, UV absorbance, and fluorescence

spectroscopic analyses of the THF-soluble part. **Figure 3.3** shows the ^1H NMR spectrum of THF-soluble poly(DBF)s prepared using BF_3-OEt_2 **(run 10 in Table 3.1)** and using CH_3SO_3H **(run 11 in Table 3.1)** along with that of fluorene as a unit model compound. In the spectra of the polymers, the aromatic proton signals appeared in the range of 4.8-7.8 ppm which are remarkably up-field shifted compared with those of fluorene (7.3 – 7.8 ppm). This remarkable magnetic anisotropy effect strongly suggests that the side-chain fluorene moieties are stacked on top of each other, i.e., the polymers have a well-controlled π-stacked conformation. It is interesting that the NMR spectrum of the polymer prepared using BF_3-OEt_2 indicates $-CH_2-$ signals in a much broader chemical shift range of 0.2-3.8 ppm than the polymer prepared using CH_3SO_3H with $-CH_2-$ signals within the range of 1.6-2.8 ppm, suggesting that the two polymers have different π-stacked structures. The spectral pattern of the polymer prepared using CH_3SO_3H is very similar to those of poly(DBF)s prepared by anionic and radical polymerizations.

It has been predicted by DFT calculations that the positions of $-CH_2-$ signals are very sensitive to main-chain conformation of poly(DBF) and that they may largely up-field shifted in a defective part in an all-trans π-stacked conformation and also in a π-stacked conformation based on alternating trans-gauche main-chain structure[7] which had never been reported for the anionic and radical polymerization products. These results suggest that cationic polymerization leads to two, different types of π-stacked conformations depending on initiator or catalyst between which one is similar to those of anionic and radical polymerization products with all-trans main-chain conformation **(Figure 3.4 a)** and the other may be a mixture of conformations including π-stacked one based on trans-gauche main-chain structure **(Figure 3.4 b)**.

Polymer conformation thus varies depending on initiator/catalyst in cationic polymerization of DBF. The difference in stereochemistry in DBF cationic polymerizations using BF_3-OEt_2 and using CH_3SO_3H may be ascribed to effects of

counter anion, i.e., $[BF_3\text{-}OH]^-$ for the system with $BF_3\text{-}OEt_2$ and $CH_3SO_3^-$ for the system with CH_3SO_3H. Counter ion effects on stereochemistry of cationic vinyl polymerization have been suggested in only very limited cases.[24,25]

It is also noteworthy that the polymer prepared using $BF_3\text{-}OEt_2$ has much broader peak shapes in the entire chemical shift range **(Figure 3.3 b)** while the one synthesized using CH_3SO_3H has rather sharp signals **(Figure 3.3 c)** which are very similar to those of soluble poly(DBF)s prepared by anionic and radical polymerizations [7,21] in spite of the fact that the two polymers have similar Mn's as revealed by SEC. Masses may be largely different leading to different spin relaxation times in NMR experiments. The conformation of the polymer prepared with CH_3SO_3H may be much more rigid leading to a much shorter spin relaxation time compared with the all-trans, π-stacked polymer prepared with $BF_3\text{-}OEt_2$.

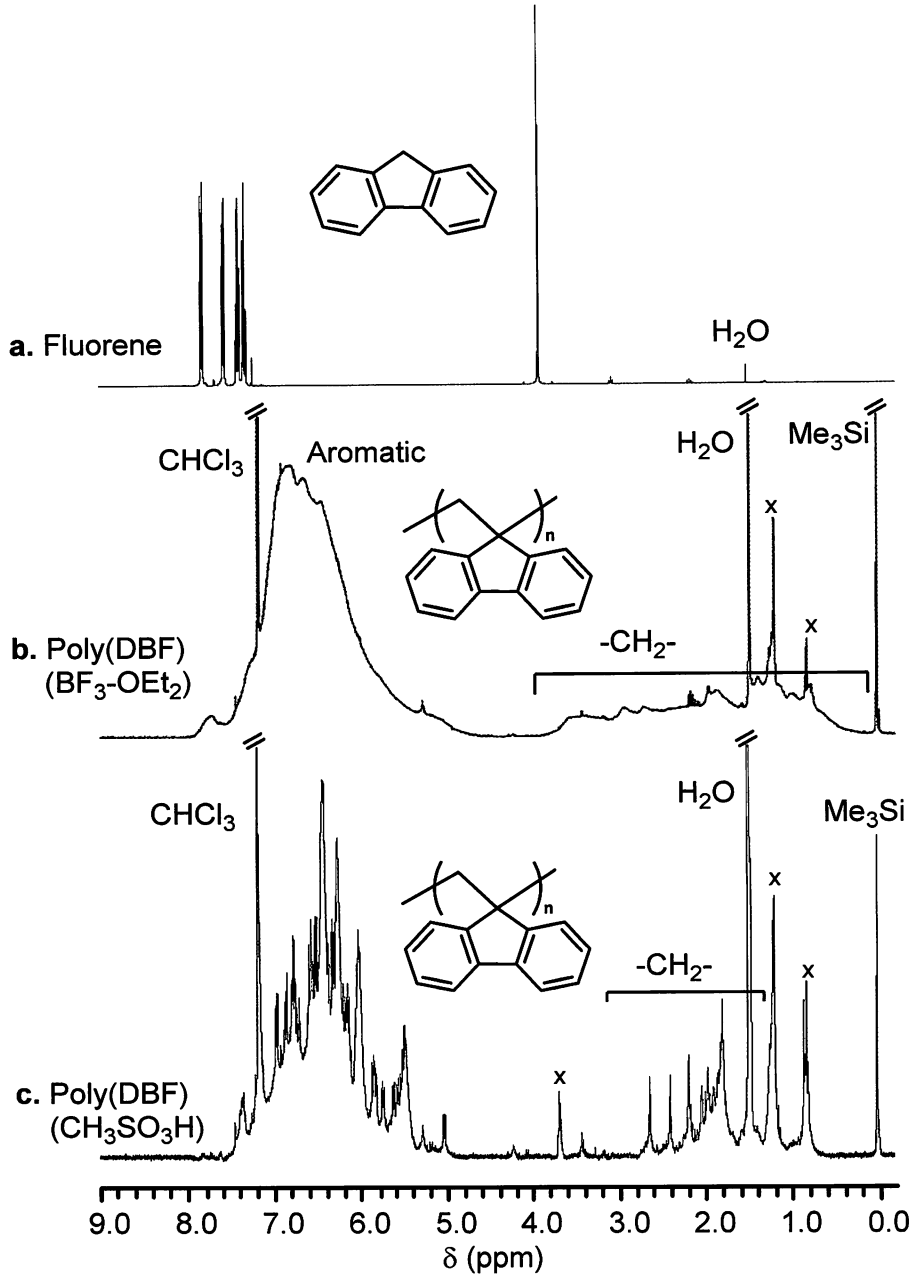

Figure 3.3 ^{1}H NMR spectra of fluorene as unit model compound (a), THF-soluble poly(DBF) prepared by cationic polymerization using BF_3-OEt_2 in CH_2Cl_2 at -40°C under the conditions same as those in **run 10 in Table 3.1** using 851mg (4.78 mmol) of DBF (b) and THF-soluble poly(DBF) prepared by cationic polymerization using CH_3SO_3H in CH_2Cl_2 at 0°C **(run 11 in Table 3.1)** (c). X denotes impurity. [400 MHz, CDCl3, room temperature].

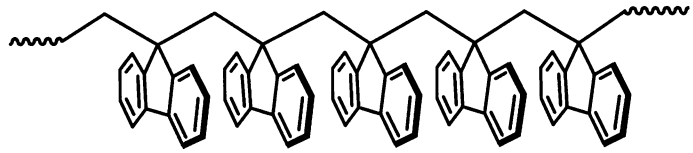

a. All trans π-stacked conformation

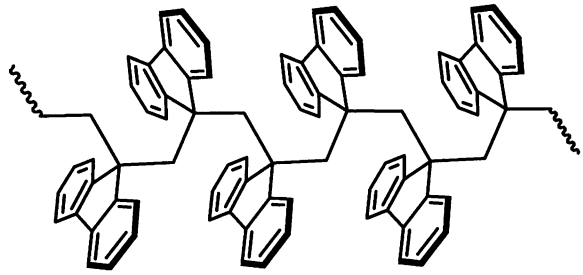

b. Trans-gauche π-stacked conformation

Figure 3.4. Proposed π-stacked conformations based on all trans main chain structure (a) and trans-gauche main chain structure (b).

Stability of the new conformation of the polymer prepared using BF_3-OEt_2 was assessed by heating the polymer in solution **(Figure 3.5)**. ^1H NMR spectral pattern did not change through heating a polymer solution in $CDCl_3$ at 60°C for 6 h, indicating that the conformation was stable under these conditions. This finding is interesting in connection to stability test of a trans-gauche, π-stacked conformation by force-field based molecular dynamics simulations which indicate that a trans-gauche conformation swiftly transforms into an all-trans conformation; reliable force-field parameters for π-stacked polymers might still need to be sought.

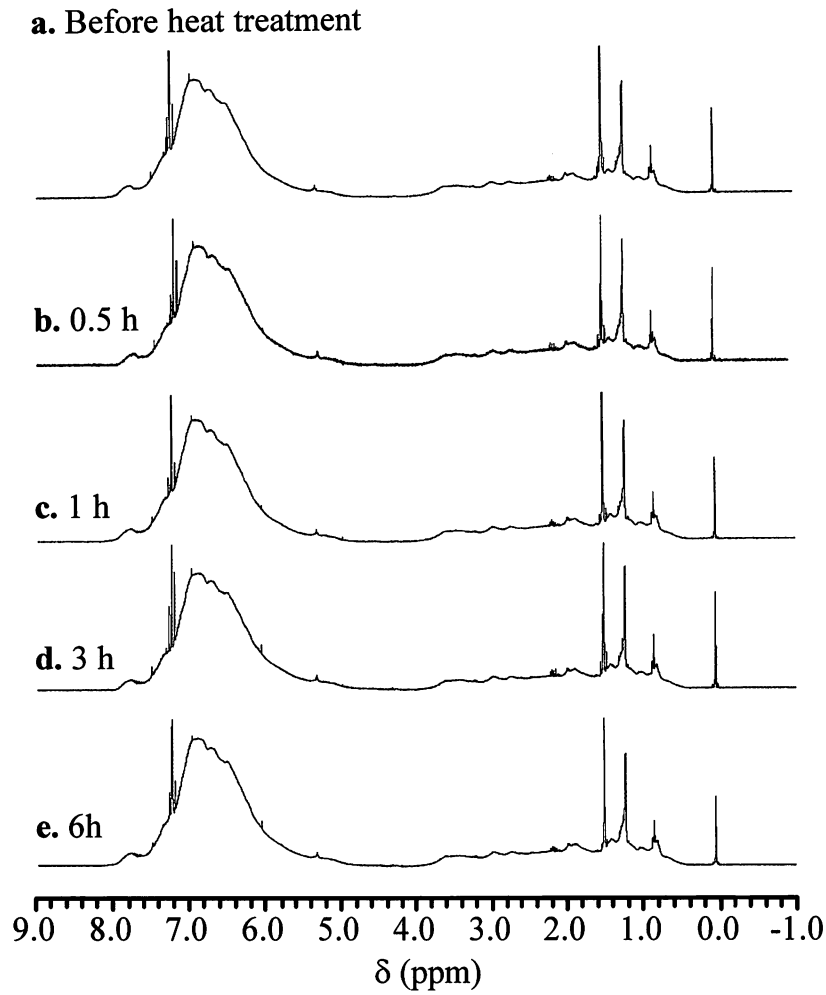

Figure 3.5 ^{1}H NMR spectra of poly(DBF) prepared using BF_3-OEt_2 **(run 10 in Table 3.1)** before (a) and after heat treatment in $CDCl_3$ solution at 60°C for 0.5 h (b), 1 h (c), 3 h (d), and 6 h (e). [400 MHz, $CDCl_3$, 23°C]

Absorbance and fluorescent spectra of the THF-soluble poly(DBF) prepared with BF_3-OEt_2 are shown in **Figure 3.6 A and B** along with those of fluorene as a unit model compound. The polymer indicated a remarkable red shifts and hypochromism with respect to fluorene in the absorbance spectrum **(Figure 3.6A)**, and it exhibited an almost exclusive dimer emission centered at around 400 nm in the emission spectrum **(Figure 3.6B)**. These results are consistent with the conclusion that the polymer has a π-stacked

conformation. The spectral shapes are similar to those reported for poly(DBF)s prepared by anionic and radical polymerizations.

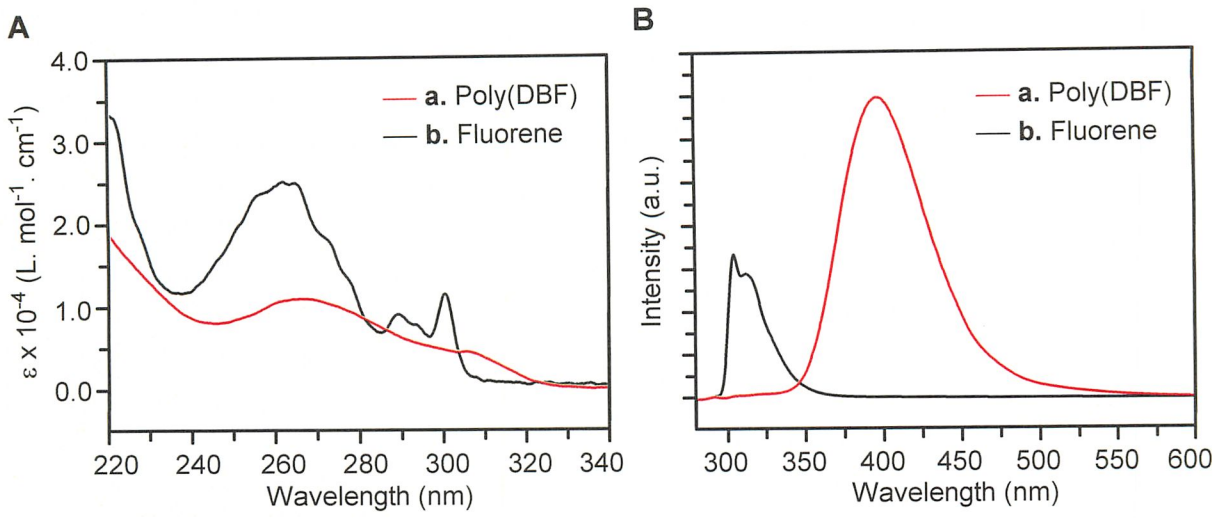

Figure 3.6 Absorbance (A) and fluorescence (B) spectra of THF-soluble poly(DBF) prepared by cationic polymerization under the conditions same as those in **run 10 in Table 3.1** using 851 mg (4.78 mmol) of DBF (a) and fluorene as a unit model (b) measured in THF. [Conditions for A; room temperature, cell path 10 mm, [fluorene] 1.00 x 10^{-5} M, [poly(DBF) (per residue)] 2.70 x 10^{-5} M: conditions for B; room temperature, cell path 10 mm, [fluorene] 1.00 x 10^{-6} M, [poly(DBF) (per residue)] 2.70 x 10^{-5} M].

Further, effects of chain length on the new π-stacked conformational were investigated using five different polymer samples obtained by preparative SEC fractionation of the THF-soluble poly(DBF) prepared using BF_3-OEt_2 at 0°C. Preparative SEC fractionation led to the samples having Mn's of 1430, 1000, 920, 820 and 740 whose Mw/Mn's were in the range of 1.0~1.1. UV and fluorescence spectra of these samples are shown in **Figure 3.7 A and B.** All samples indicated red shifts and hypochromism in absorbance spectra, and the extent of hypochromism was greater for a sample having higher Mn **(Figure 3.7A)**; this tendency is similar to that reported for poly(DBF)s prepared by anionic polymerization.[6,7] A longer chain may lead to stronger electronic

interactions between neighboring, stacked fluorene moieties in the poly(DBF) chain obtained using BF_3-OEt_2 whose conformation involves trans-gauche π-stacked structure as well as those in all-trans π-stacked poly(DBF) chain.

In the fluorescence spectra **(Figure 3.7B)**, all samples indicated spectra consisting of excimer (dimer) emission centered at around 400 nm and monomer emission centered at around 310-320 nm between which the former had much higher intensity. As for the intensity ratios between monomer and excimer emissions, no clear tendency of decrease or increase depending on Mn was found. It is noteworthy that even the oligomer sample having an Mn of 740 exhibited clear characters of π-stacked conformation in the UV and emission spectra. This may mean that the polymer prepared using BF_3-OEt_2 has a stable π-stacked conformation even when the chain is rather short.

In addition, the sample having the highest Mn of 1430 prepared at 0°C indicated the clear monomer emission **(Figure 3.7B b)** while no clear monomer emission was observed for the poly(DBF) (Mn 500) prepared at -40°C using BF_3-OEt_2 **(Figure 3.6B)**. This result indicates that the extent of π-stacked conformational control is higher at -40 °C.

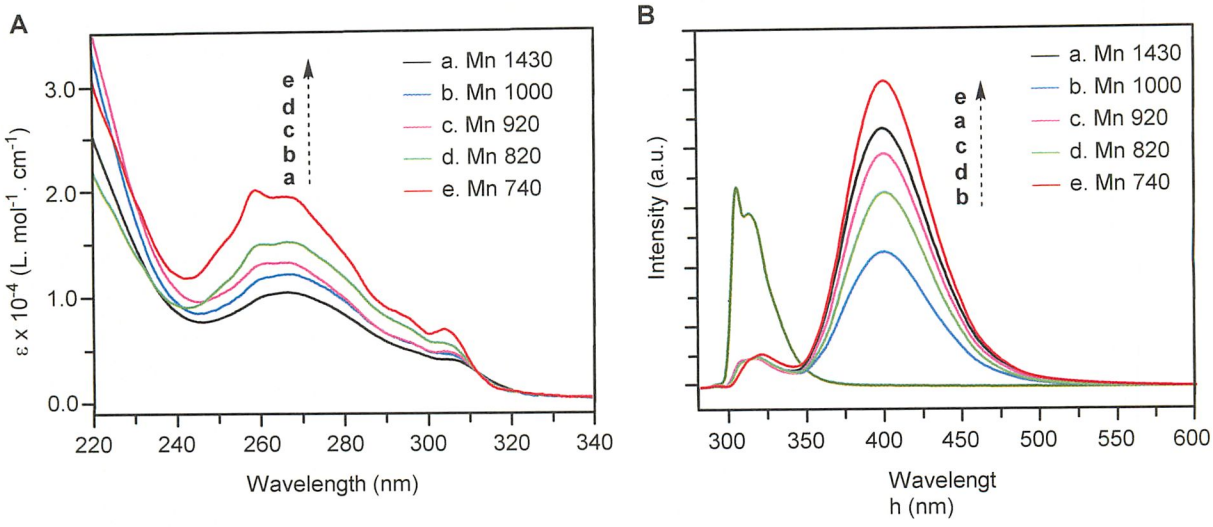

Figure 3.7. Absorbance (A) and fluorescence (B) spectra of SEC-fractionated poly(DBF)s obtained from the polymer prepared by cationic polymerization using BF_3-OEt_2 at 0°C under the conditions same as those in **run 3 in Table 3.1** using 1.26 g (7.09 mmol) of DBF: Mn 1430 (a), 1000 (b), 920 (c), 820 (d), and 740 (e). The spectra in A were normalized at 312 nm according to the spectra in ref. 7. The spectra in B were normalized at 315 nm. [room temperature, cell path 10 mm, in THF]

3.4 Conclusion

Cationic polymerization of DBF was studied under various conditions. In the polymerization using BF_3-OEt_2, both [DBF]/[BF_3] ratio and DBF concentration appeared to affect chain length of the products. In addition to BF_3-OEt_2, CH_3SO_3H, CF_3CO_2H, and CH_3CO_2H led to polymers. The fact that the three protonic acids can lead to poly(DBF) indicates that DBF is a highly reactive monomer in cationic polymerization. The cationic polymerization products were found to have well controlled π-stacked conformations which may vary depending on initiator or catalyst. The polymer obtained using BF_3-OEt_2 is proposed to possess a π-stacked conformation based on trans-gauche main chain at least in part while the one prepared using CH_3SO_3H has a π-stacked conformation based on all-trans main chain. There results may arise from stereochemical effects of counter anion through cationic polymerization.

These features are in a sharp contrast to the facts that counter anion effects have been noticed in only in limited cases of cationic vinyl polymerization and that the extent of stereo control in cationic polymerization of vinyl monomers is generally rather moderate. In addition, even rather short chains prepared with BF_3-OEt_2 were confirmed to have a stable π-stacked conformation. This work hence clearly demonstrated that cationic polymerization is not just an alternative, effective method to prepare all-trans π-stacked poly(DBF) but also is a method to lead to a novel π-stacked conformation contributed by trans-gauche main chain.

3.5 References

1 E. Yashima, K. Maeda, H. Iida, Y. Furusho and K. Nagai, Helical polymers: synthesis, structures, and functions, Chem. Rev., 2009, **109**, 6102-6211.

2 E. Yashima, N. Ousaka, D. Taura, K. Shimomura, T. Ikai and K. Maeda, Supramolecular helical systems: helical assemblies of small molecules, foldamers, and polymers with chiral amplification and their functions, Chem. Rev., 2016, **116**, 13752−13990.

3 Y. Okamoto and T. Nakano, Asymmetric polymerization, Chem. Rev., 1994, **94**, 349-372.

4 T. Nakano and Y. Okamoto, Chem. Rev., Synthetic helical polymers: conformation and function, 2001, **101**, 4013-4038.

5 a) T. Nakano, Synthesis, structure and function of π-stacked polymers, Polym. J., 2010, **42**, 103-123. b) T. Nakano, π-Stacked polymers and molecules, Springer, Tokyo, 2016.

6 T. Nakano, K. Takewaki, T. Yade and Y. Okamoto, Dibenzofulvene, a 1,1-diphenylethylene analogue, gives a π-stacked polymer by anionic, freeradical, and cationic catalysts, J. Am. Chem. Soc., 2001, **123**, 9182-9183.

7 T. Nakano and T. Yade, Synthesis, structure, and photophysical and electrochemical properties of a π-stacked polymer, J. Am. Chem. Soc., 2003, **125**, 15474-15484.

8 T. Nakano, O. Nakagawa, M. Tsuji, M. Tanikawa, T. Yade and Y. Okamoto, Poly(2,7-di-n-pentyldibenzofulvene) showing chiroptical properties in the solid state based purely on a chiral conformation, Chem. Commun., 2004, 144-145.

9 K. Watanabe, T. Sakamoto, M. Taguchi, M. Fujiki and T. Nakano, A chiral π-stacked vinyl polymer emitting white circularly polarized light, Chem. Commun., 2011, **47,** 10996-10998.

10 P. G. Gudeangadi, T. Sakamoto, Y. Shichibu, K. Konishi and T. Nakano, Chiral polyurethane synthesis leading to p-stacked 2/1-helical polymer and cyclic compounds, ACS Macro Letters, 2015, **4,** 901-906.

11 M. Merlani, Y. Koyama, H. Sato, L. Geng, V. Barbakadze, B. Chankvetadze and T. Nakano, Ring-opening polymerization of a 2,3-disubstituted oxirane leading to a polyether having a carbonylearomatic π-stacked structure, Polym. Chem., 2015, **6,** 1932-1936.

12 W. Yang and T. Nakano, Synthesis of poly(1,10-phenanthroline-5,6-diyl)s having a π-stacked, helical conformation, Chem. Commun., 2015, **51**, 17269-17272.

13 H. Wang, Y. Wang, X. Ye, H. Hayama, H. Sugino, H. Nakano and T. Nakano, π-Stacked poly(vinyl ketone)s with accumulated pushepull triphenylamine moieties in the side chain, Polym. Chem., 2017, **8,** 708–714.

14 A. Cappelli, S. Galeazzi, G. Giuliani, M. Anzini, M. Aggravi, A. Donati, L. Zetta, A. C. Boccia, R. Mendichi, G. Giorgi, E. Paccagnini and S. Vomero, Anionic polymerization of a benzofulvene monomer leading to a thermoreversible π-stacked polymer. studies in macromolecular and aggregate structure, Macromolecules, 2008, **41**, 2324-2334.

15 A. Cappelli, V. Razzano, M. Paolino, G. Grisci, G. Giuliani, A. Donati, R. Mendichi, F. Samperi, S. Battiato, A. C. Boccia, A. Mura, G. Bongiovanni, W. Mroz and C. Botta, Bithiophene-based polybenzofulvene derivatives with high stacking and hole mobility, Polym. Chem., 2015, **6**, 7377–7388.

16 S. P. Jagtap and D. M. Collard, 2D π-stacked conjugated polymers based on pseudo-geminal disubstituted [2.2]paracyclophane, J. Am. Chem. Soc., 2010, **132**, 12208–12209.

17 K. M. Knoblock, C. J. Silvestri and D. M. Collard, Stacked conjugated oligomers as molecular models to examine interchain interactions in conjugated materials, J. Am. Chem. Soc., 2006, **128**, 13680-13681.

18 F. Salhi and D. M. Collard, π-Stacked conjugated polymers: the influence of paracyclophane π-stacks on the redox and optical properties of a new class of broken conjugated polythiophenes, Adv. Mater., 2003, **15**, 81-85.

19 Y. Morisaki and Y. Chujo, Through-space conjugated polymers based on cyclophanes, Angew. Chem. Int. Ed., 2006, **45**, 6430-6437.

20 T. Nakano, T. Yade, M. Yokoyama and N. Nagayama, Charge transport in a π-stacked poly(dibenzofulvene) film, Chem. Lett., 2004, **33**, 296-297.

21 T. Nakano, T. Yade, Y. Fukuda, T. Yamaguchi and S. Okumura, Free-radical polymerization of dibenzofulvene leading to a π-stacked polymer: structure and properties of the polymer and proposed reaction mechanism, macromolecules, 2005, **38**, 8140-8148.

22 G. I. Almerindo, D. W. Tondo and J. R. Pliego, Ionization of organic acids in dimethyl sulfoxide solution: a theoretical ab initio calculation of the pK_a using a new parametrization of the polarizable continuum model, J. Phys. Chem. A, 2004, **108,** 166-171.

23 F. G. Bordwell, Equilibrium acidities in dimethyl sulfoxide solution, Acc. Chem. Res., 1988, **21**, 456-463.

24 T. Kunitake, K. Takarabe and S. Tsugawa, The Counterion effect on the steric course of the cationic polymerization of isobutyl vinyl ether, Polym. J., 1976, **8**, 363–368.

25 S. J. Mumby and M. S. Beevers, Dielectric and ^{13}C n.m.r, studies of various stereostructural forms of poly(N-vinyl carbazole), Polymer, 1985, **26**, 2014-2020.

Chapter 4

Solid-state Structure of π-Stacked Poly(dibenzofulvene)

4.1. Introduction

Conformation of single polymer chain is a determinant of properties of a polymer as an isolated chain while structure of a solid material as a group of many chains is also an important aspect from a view of polymeric materials. As for poly(DBF), detailed chain conformation has been established for single-chain species using soluble oligomers while polymerization of DBF by anionic, radical, and cationic polymerizations lead to mostly solvent-insoluble materials.[1-4] It has been established that soluble and insoluble poly(DBF)s have the same chemical structure by means of IR spectroscopy.[1] In addition, insoluble poly(DBF) has been proposed to involve longer chains than the soluble poly(DBF).[2] The formation of the insoluble fraction is considered to be facilitated by inter-molecular interaction which would be more significant for longer chains.

In this work, solid-state structure of tetrahydrofuran (THF)-insoluble poly(DBF) was studied by various methods using the samples obtained by prepared polymerization, the most conventional method of vinyl polymer synthesis.

4.2 Experimental

4.2.1 Materials

DBF was prepared according to the literature.[1,2] α,α'-Azobis(isobutyronitrile) (AIBN) was recrystallized from an ethanol solution. Hexane, methanol, chloroform, and benzene for radical polymerization were purified by distilled and stored under a N_2 atmosphere. The other solvents were purified by the usual methods, degassed under vacuum and flashed with N_2, and stored under a N_2 atmosphere.

4.2.2 Instrumentation

NMR spectra were recorded on a JEOL JMN-ECX400 spectrometer. Size-exclusion chromatography (SEC) measurements were carried out using a chromatographic system consisting of a JASCO DG-980-50 degasser, a HITACHI L-7100 pump, a HITACHI L-7420 UV-Vis detector and a HITACHI L-7490 IR detector, equipped with TOSOH TSKgel G3000H HR and G6000H HR columns (30 × 0.72 (i.d.) cm) connected in series (eluent: THF, flow rate: 1.0 mL/min). UV-Vis spectra were taken on JASCO V-550 and V-570 spectrophotometers, and fluorescence spectra were measured on a JASCO PF-8500 fluorescence spectrophotometer. Thermal analysis was conducted using RIGAKU Thermo Plus DSC8230 and TG8120. Scanning electron microscopy (SEM) images were obtained a JEOL JSM-7400F microscope with an LEI detector at an acceleration voltage of 3.0 kV and a working distance of 6.0 mm, and the samples were coated with Pt using a JEOL JFC-1600 Auto Fine Coater (30 mA, 20 sec). Transmission electron microscopy (TEM) analysis was performed using a JEOL JEM-2100F microscope equipped with a CCD image sensor at an acceleration voltage of 200 kV using a collodion film sample support. X-ray diffraction (XRD) profiles were obtained using a Rigaku MiniFlex300 diffractometer with monochromated Cu-Kα radiation. A Surface area of the polymers were measured by nitrogen sorption using an Autosorb 6AG (Quantachrome), and determined by Brunauer-Emmett-Teller (BET) equation.

4.2.3 Radical polymerization

The radical polymerizations were carried out in a flask sealed with a glass-made three-way stopcock. The joint was sealed with high-vacuum grease. A typical procedure is described for **run 1 in Table 4.1**. DBF (1859.8 mg, 10.44 mmol) and AIBN (21.4 mg, 0.13 mmol) were placed in a 50-mL flask, and the flask was evacuated for 5 min at room temperature and flashed with dry N_2 gas. Hexane (24.2 mL) was added using a syringe, and the monomer and the initiator were completely dissolved. The

polymerization was initiated by heating the solution at 60 °C, and the reaction mixture was cooled at 0 °C after 24 h of heating. An aliquot (about 0.1 mL) of the solution part of the reaction mixture was transferred to an NMR sample tube (5 mm diameter), 0.6 mL of $CDCl_3$ was added, and the resulting diluted solution was subjected to ^1H NMR analysis. Comparison of the intensity of the vinyl proton signals of remaining DBF (s, 6.0 ppm) with that of the benzene signal (s, 7.4 ppm) as an internal standard gave a monomer consumption ratio of 83 %. After removing the solvents from the rest of the reaction mixture, the residue was separated into tetrahydrofuran (THF)-soluble and -insoluble parts with a centrifuge.

4.3. Results and Discussion

4.3.1. Sample preparation by radical polymerization

In order to obtain samples of poly(DBF), radical polymerization was conducted in hexane, methanol, chloroform, and benzene using AIBN as initiator at 60°C under N_2 atmosphere according to the literature[3] (**Table 4.1**). The reactions led to high conversion ratio of DBF in most cases, and THF-insoluble materials were obtained by fractionation with a centrifuge. Mn's of the THF-soluble parts were less than 1,100, confirming that poly(DBF) has a high tendency to form insoluble materials where the chains would strongly interact with each other.

Table 4.1. Radical polymerization of DBF in various solvents using AIBN at 60°C

Run	[I] (M)	[M]/[I]	Conversion[e] (%)	THF-insol. Part (%)	THF-soluble part (%)	THF-sol. Part		
						Mn[f]	Mw/Mn	Mp
1[a]	0.005	80	83	63	25	859	1.096	802
2[b]	0.005	80	73	48	51	412	1.000	909
3[c]	0.005	80	>99	14	86	561	1.035	497
4[d]	0.005	80	>99	85	15	1066	3.486	584

[a]DBF (1859.8 mg, 10.44 mmol), [b](1887.6g, 10.60 mmol), [c](801.0 mg, 4.50 mmol), [d] (1820.4 mg, 10.22 mmol); [e]Determined on the basis of ^{1}H NMR analysis of crude products; [d]Determined by SEC using polystyrene standards; [f] Mn values relative to standard polystyrenedetermined by SEC.

4.3.2. Thermal properties

Figure 4.1 shows the profiles of TGA (thermo gravimetry analysis) and DTA (differential thermal analysis) for the THF-insoluble poly(DBF) samples prepared by radical polymerization. The polymers indicated an onset temperature of decomposition in the range of ca. 260-280°C.

In addition, the polymers prepared by radical polymerization exhibited transitions at around 160-170°C with very clear signals for the polymers prepared by radical polymerization. The transitions at 160-170°C are considered to be based on the detachment of DBF monomer from the chain terminal through depolymerization. This has been supported by an independent experiment conducted by Mr. Jiyuie Luo and Prof. Tamaki Nakano (Hokkaido University); they confirmed the presence of a significant amount of DBF monomer by ^{1}H NMR analyses on the product which had been heated to 180°C. The endothermic transitions in **Figure 4.1** A, C, and D mean that detachment of DBF monomer form a chain (depolymerization) is an endothermic reaction while the exothermic transitions in **Figure 4.1** B may mean that detached DBF monomer crystallized exothermically in situ.

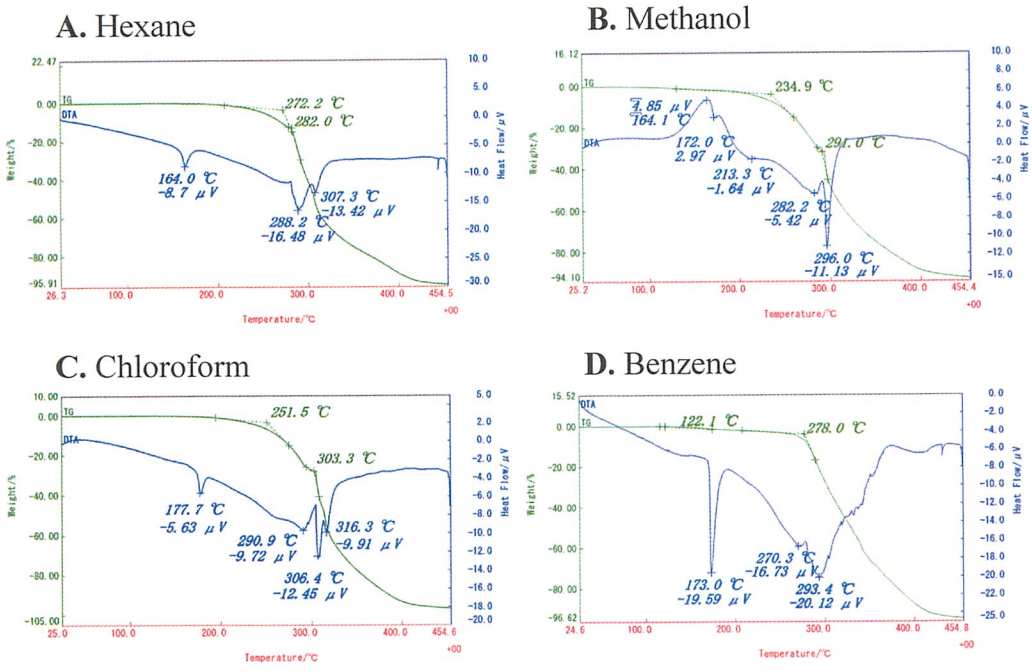

Figure 4.1. TGA and DTA profiles of THF-insoluble poly(DBF)s prepared by radical polymerization.

4.3.2. XRD profiles

Figure 4.2 indicates the XRD profiles of the THF-insoluble poly(DBF)s prepared by radical polymerization. All polymers, regardless of how they were synthesized, exhibited clear reflections at 2θ = 6.5, 11.0, 19.4, 24.1, and 26.7 degrees which correspond to d-spacing values of 13.4, 8.04, 4.57, 3.69, and 3.35 angstroms, respectively. The d-spacing values of 4.57, 3.69, and 3.35 angstroms may be ascribed to intra-chain π-stacking between side-chain fluorene moieties; π-stacking in the solid state may have at least three typical forms due to chain packing. On the other hand, the d-spacing values of 13.4 and 8.04 angstroms are too long to be ascribed to any intra-chain ordering, and they would be more reasonably ascribed to inter-chain ordering. Although the exact structures of inter-chain ordering in the solid state is not yet clear at this point, it would be imagined that two poly(DBF) chains may tangle on each other to

form a structure where two chains forming a double helix or a structure like a chain carrying another chain on its back.

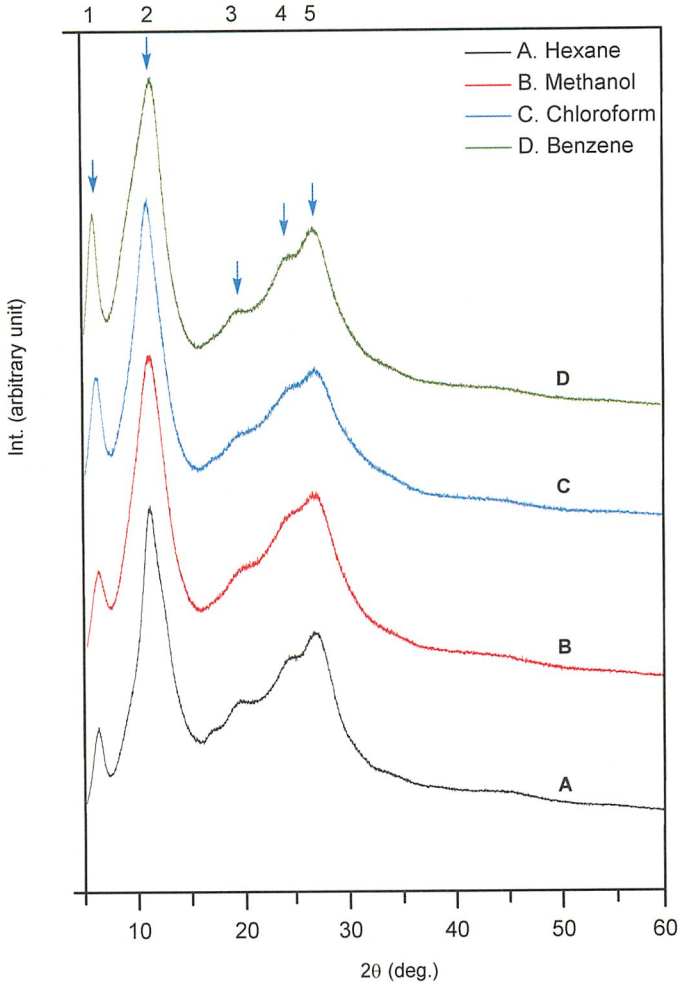

Figure 4.2. XRD profiled of THF-insoluble poly(DBF) prepared by radical polymerization in hexane (A), methanol (B), chloroform (C), and benzene (D).

4.3.3. Microscopic analysis

The THF-insoluble polymers were analyzed by SEM and TEM (**Figures 4.3** and **4.4**). **Figure 4.3** shows the SEM images of the polymers; the polymers did not show flat surface images and indicated rough which are indicative of rather porous structure. In addition, the image varied depending on polymerization solvent, suggesting that solid-state morphology of poly(DBF) may change due to difference in solvent properties.

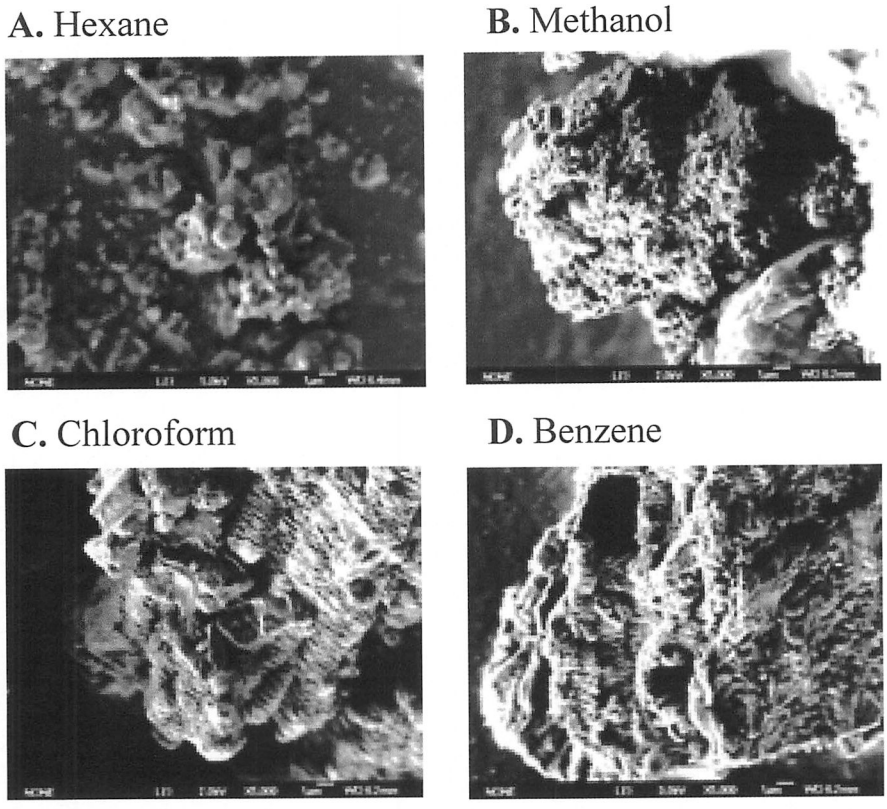

Figure 4.3. SEM images of THF-insoluble poly(DBF)s by radical polymerization in hexane (A), methanol (B), chloroform (C), and benzene (D).

Figure 4.4 shows the TEM images of the polymers prepared in hexane, and MeOH. All images in the figures exhibit very fine structures whose sizes may be approximately similar to those of single chains of poly(DBF). The images may support alignments of poly(DBF) chains in the solid state although the image resolution is not high enough to allow precise determination of chain size and inter-chain spacing. Images with higher resolution will be indispensable in clarifying further details of solid-state structure of poly(DBF). Nevertheless, the image of the polymer made in MeOH may appear to represent finer structures. The insoluble poly(DBF) may have different, fine and ordered chain orientations depending of polymerization solvent.

A. Polymerization in hexane

B. Polymerization in MeOH

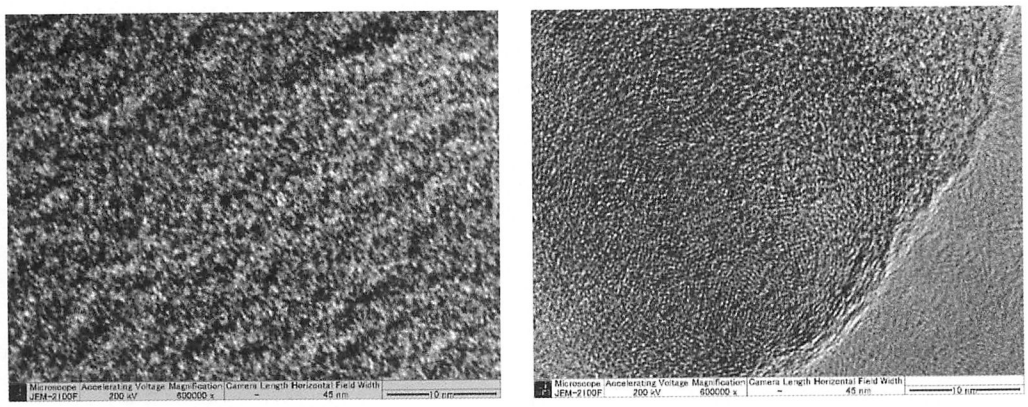

Figure 4.4 TEM images of THF-insoluble poly(DBF)s prepared in hexane (A) and in MeOH (B).

4.3.4 Surface area analysis

Surface areas of the THF-insoluble poly(DBF) samples were estimated by nitrogen gas absorption on the basis of the Brunauer–Emmett–Teller (BET) theory.[5] The surface areas of the polymers prepared in hexane, methanol, chloroform, and benzene were 4.10 m^2/g with total pore volume = 0.006058 cc/g for pores smaller than 931.7 Å (diameter), 11.63 m^2/g with total pore volume = 0.1593 cc/g for pores smaller than 2197.1 Å (diameter), 29.00 m^2/g Total pore volume = 0.1178 cc/g for pores smaller than 1263.6 Å (diameter), and 3.95 m^2/g with Total pore volume = 0.009931 cc/g for pores smaller than 837.4 Å (diameter), respectively. These surface areas were less than that of non-porous polystyrene samples (29 m^2/g);[6] poly(DBF)s as they are would not fall into categories of porous materials. However, since the solid-state structure of poly(DBF)s seem to vary both at the levels of nanometer and micrometer on the basis of the SEM and TEM results, the observed variation of surface area could arise from a structure composed of a few chains or from a structure composed of a much greater numbers of

chains. In either case, further polymer designs including those of poly(DBF) derivatives from a wide view encompassing molecular aggregation of a few chains through nano~micro particle formation will be necessary in obtaining a poly(DBF)-based organic material having a larger surface area which may be used as catalysis support.

4.4. Conclusions

Solid-state structures of insoluble poly(DBF) were studied by thermal analysis, powder x-ray diffraction, BET-theory-based N_2 gas absorption analysis, SEM and TEM. The XRD patterns and TEM results suggest that chain ordering is present in the solid-state samples of poly(DBF) in the solid state. The solid-state structure may vary depending on polymerization solvent as implied by the SEM images. Although surface areas of the poly(DBF) samples were smaller than that of non-porous polystyrene as indicated by the gas absorption analysis, it could be improved by altering the polymer structure especially by introducing side-chains at the 2- and 7-positions of fluorene backbone of monomeric units. Further, the chain ordering could be utilized as sterically confined reaction space for catalysis if proper metallic species are chemically or physically bound to the surface of insoluble polymer.

4.5. References

1 T. Nakano, K. Takewaki, T. Yade and Y. Okamoto, Dibenzofulvene, a 1, 1-diphenylethylene analogue, gives a π-stacked polymer by anionic, free-radical, and cationic catalysts, J. Am. Chem. Soc, 2001, **123,** 9182-9183.

2 T. Nakano and T. Yade, Synthesis, structure, and photophysical and electrochemical properties of a π-stacked polymer, J. Am. Chem. Soc., 2003, **125**, 15474-15484.

3 T. Nakano, T. Yade, Y. Fukuda, T. Yamaguchi and S. Okumura, Free-radical polymerization of dibenzofulvene leading to a π-stacked polymer: structure and properties of the polymer and proposed reaction mechanism, Macromolecules, 2005, **38**, 8140-8148.

4 H. Nageh, Y. Wang and T. Nakano, Cationic polymerization of dibenzofulvene leading to a π-stacked polymer, Polymer, 2018, **144**, 51-56.

5 S. Brunauer, P. H. Emmett and E. Teller, Adsorption of gases in multimolecular layers, J. Am. Chem. Soc., 1938, **60**, 309-319.

6. S. Longo, J. G. Vitillo, C. Daniel and G. Guerra, Monolithic aerogels Based on poly (2, 6-diphenyl-1, 4-phenylene oxide) and syndiotactic polystyrene. ACS Appl. Mater. Interfaces, 2013, **5**, 5493-5499.

List of publication

1) Photo-induced β-elimination of 9-fluorenylmethanol leading to dibenzofulvene

H. Nageh, L. Zhao, A. Nakayama, J. Y. Hasegawa, Y. Wang and T. Nakano, *Chem. Commun.*, **2017**, *53*, 8431-8434.

2) Cationic polymerization of dibenzofulvene leading to a π-stacked polymer

H. Nageh, Y. Wang and T. Nakano, *Polymer*, **2018**, *144*, 51-56.

Acknowledgment

I would like to express my appreciation beyond words to my supervisor, Prof. Dr. Tamaki Nakano who guided in my thesis program and continuously provided me with stimulating ideas on science, life and warm encouragement.

I gratefully acknowledge Prof. Dr. Takanori Suzuki, Prof. Dr. Shin Mukai, and Prof. Dr. Masaya Sawamura for their reviewing my thesis and giving me helpful advises on it.

I express my gratitude to Prof. Dr. Jun-ya Hasegawa and Dr. Akira Nakayama and Ms. Liming Zhao of Hasegawa group for their kind collaboration and helpful advice and to Prof. Dr. Naofumi Naga of Shibaura Institute of Technology for his valuable comments on the thesis work.

I am thankful to Dr. Yue Wang of Nakano Laboratory for her experimental assistance and wish to thank all members of Nakano Laboratory of Hokkaido University for their friendship and encouragement.

My stay in Hokkaido University was fully supported by "Advanced Graduate School (AGS)" scholarship from the university sponsored by The Government of Japan through a MEXT scholarship. I herewith express my sincere appreciation to the nation of Japan for their generous financial support for my stay and studies at Hokkaido University.

Finally, I acknowledge my beloved parents, Nageh Anwar and Kawthar Hamed, and all family members for encouragement and support.

Hassan Nageh
2018/9/26